This is a repository copy of *Self-organization of rectangular bipyramidal helical columns by supramolecular orientational memory epitaxially nucleated from a Frank-Kasper σ phase*.

White Rose Research Online URL for this paper:
https://eprints.whiterose.ac.uk/180594/

Version: Published Version

Article:

Percec, V., Huang, N., Xiao, Q. et al. (8 more authors) (2022) Self-organization of rectangular bipyramidal helical columns by supramolecular orientational memory epitaxially nucleated from a Frank-Kasper σ phase. Giant, 9. 100084. ISSN 2666-5425

https://doi.org/10.1016/j.giant.2021.100084

Reuse
This article is distributed under the terms of the Creative Commons Attribution-NonCommercial-NoDerivs (CC BY-NC-ND) licence. This licence only allows you to download this work and share it with others as long as you credit the authors, but you can't change the article in any way or use it commercially. More information and the full terms of the licence here: https://creativecommons.org/licenses/

Takedown
If you consider content in White Rose Research Online to be in breach of UK law, please notify us by emailing eprints@whiterose.ac.uk including the URL of the record and the reason for the withdrawal request.

eprints@whiterose.ac.uk
https://eprints.whiterose.ac.uk/

Giant, 9, 2022, 100084

ELSEVIER

GIANT

Check for updates

Full-length article

Self-organization of rectangular bipyramidal helical columns by supramolecular orientational memory epitaxially nucleated from a Frank-Kasper σ phase

Virgil Percec[a,*], **Ning Huang**[a], **Qi Xiao**[a], **Benjamin E. Partridge**[a], **Dipankar Sahoo**[a], **Mohammad R. Imam**[a], **Mihai Peterca**[a], **Robert Graf**[b], **Hans-Wolfgang Spiess**[b], **Xiangbing Zeng**[c], **Goran Ungar**[c,d]

[a] Roy and Diana Vagelos Laboratories, Department of Chemistry, Roy and Diana Vagelos Laboratories, University of Pennsylvania, Philadelphia, PA 19104-6323, United States
[b] Max-Planck Institute for Polymer Research, Mainz 55128, Germany
[c] Department of Materials Science and Engineering, University of Sheffield, Sheffield S1 3JD, United Kingdom
[d] State Key Laboratory for Mechanical Behavior of Materials, Xi'an Jiaotong University, Xi'an 710049, China

Keywords: Fiber X-ray diffraction, Epitaxial nucleation, Supramolecular, Self-assembly, Soft matter, Dendrimers

Programming living and soft complex matter via primary structure and self-organization represents the key methodology employed to design functions in biological and synthetic nanoscience. Memory effects have been used to create commercial technologies including liquid crystal displays and biomedical applications based on shape memory polymers. Supramolecular orientational memory (SOM), induced by an epitaxial nucleation mediated by the close contact spheres of cubic phases, emerged as a pathway to engineer complex nanoscale soft matter of helical columnar hexagonal arrays. SOM preserves the crystallographic directions of close contact supramolecular spheres from the 3D phase upon cooling to the columnar hexagonal periodic array. Despite the diversity of 3D periodic and quasiperiodic nanoarrays of supramolecular dendrimers, including Frank-Kasper and quasicrystal, all examples of SOM to date were mediated by $Im\bar{3}m$ (body-centered cubic, BCC) and $Pm\bar{3}n$ (Frank-Kasper A15) cubic phases. Expanding the scope of SOM to non-cubic arrays is expected to generate additional morphologies that were not yet available by any other methods. Here we demonstrate the SOM of a dendronized triphenylene that self-organizes into helical columnar hexagonal and tetragonal $P4_2/mnm$ (Frank-Kasper σ) phases. Structural analysis of oriented fibers by X-ray diffraction reveals that helical columnar hexagonal domains self-organize an unusual rectangular bipyramidal morphology upon cooling from the σ phase. The discovery of SOM in a non-cubic Frank-Kasper phase indicates that this methodology may be expanded to other periodic and quasiperiodic nanoarrays organized from self-assembling dendrimers and, most probably, to other soft and living complex matter.

2666-5425/© 2021 Published by Elsevier Ltd. This is an open access article under the CC BY-NC-ND license (http://creativecommons.org/licenses/by-nc-nd/4.0/) https://doi.org/10.1016/j.giant.2021.100084

Full-length article

Introduction

Complex nanoscale living and soft-matter relies on a broad range of organic matter that is self-organized across multiple length scales [1–12]. Programmed memory effects in complex soft matter have provided a convenient route to access unprecedent morphologies. Shape memory has been extensively explored for biomedical applications [13,14] and molecular machines [15,16], while orientational memory in liquid crystals is ubiquitous in modern display devices [17]. Chiral memory effects have been investigated in molecular and supramolecular systems [18–21]. Epitaxially nucleated supramolecular orientational memory (SOM) was recently discovered as a methodology to generate otherwise inaccessible nanoscale architectures of columnar arrays generated from self-assembling dendrons and dendrimers [22–26]. SOM requires that self-organized soft matter undergoes a reversible phase transition between a 2D or 3D columnar hexagonal (Φ_h) phase (*p*6mm space group) and a 3D phase self-organized from supramolecular spheres that may in fact be supramolecular polygonal objects [4,5]. For simplicity, in this manuscript as in the previous SOM publications [22–26] they will be considered to be spheres. Upon cooling from a 3D phase of spheres, the hexagonal domains of supramolecular columns are oriented by an epitaxial nucleation induced by the closest contact crystallographic directions in the preceding 3D phase, thus "remembering" these directions in the Φ_h array. Briefly, the SOM epitaxy follows the close contact sphere directions of the cubic phase. "Close contact" can be defined as the spheres with the smallest inter-sphere distances in a lattice. This distance is smaller than the diameter of the theoretical spherical objects. A wide range of morphologies, including orthogonal [22], tetrahedral [23,24], distorted dodecahedral [25], and rhombitruncated cuboctahedral [26] arrangements of helical columnar hexagonal arrays have been achieved by utilizing SOM along the different close contact directions in $Pm\bar{3}n$ (A15 Frank-Kasper) [27–42] and $Im\bar{3}m$ (BCC) [43,44] cubic phases [21–26].

The architectures realized *via* SOM have all been, so far, generated from cubic phases of self-organizable dendrimers. However, complex soft-matter organizes into a large diversity of 3D Frank-Kasper phases [45,46] generated from supramolecular spheres, including tetragonal $P4_2/mnm$ (Frank-Kasper σ), 12-fold liquid quasicrystal (LQC), the Frank-Kasper Z phase, and Laves phases. Though some of them (A15 [27–42], σ [47], LQC [48–50]) were first discovered in synthetic soft matter for libraries [4–10,27–44,47–86] of self-assembling dendrons, dendrimers and dendronized polymers, they have since been simulated, explained computationally [87–89] and observed also in block copolymers [90–96], surfactants [97–100], dendron-like silsesquioxane-cage molecules [101–106], lipids [107–114], nanoparticles [115,116], DNA-nanoparticle conjugates [117], and sugar-polyolefin [118,119] block-copolymer-generated spherical nanoparticles, and colloidal crystals [120–122]. Therefore, since Frank-Kasper phases are broadly encountered not only in the field of supramolecular dendrimers but also of block copolymers, surfactants, biological molecules and of other self-assembling molecules their SOM represents a fundamental problem, that in our opinion, must be elucidated. The prevalence of Frank-Kasper phases in soft matter raises the fundamental question: can SOM be mediated by non-cubic 3D phases generated from supramolecular spheres? While a simple answer would be yes, a more complex question is what is their resulting morphology?

In this report we demonstrate a SOM between a tetragonal $P4_2/mnm$ (Frank-Kasper σ) phase and helical columnar hexagonal arrays self-organized from a triphenylene dendronized with first-generation self-assembling dendrons, (3,4,5)12G1-Tp. As with all previous examples of SOM, cooling from the 3D phase generated from supramolecular spheres produces a nanoscale architecture of columnar hexagonal domains. Structural analysis of aligned fiber X-ray diffraction (XRD) reveals that the non-cubic symmetry of the $P4_2/mnm$ phase mediated epitaxial alignment along the close contact $[002]_{tet}$, $[410]_{tet}$, and equivalent $[140]_{tet}$ directions. Due to the complexity of the $P4_2/mnm$ unit cell, which contains 30 supramolecular spheres, two alternative pathways for the SOM effect along the $[410]_{tet}$ direction are discussed and discriminated using XRD performed on oriented fiber samples. The resulting nanoscale morphology exhibits an unusual rectangular bipyramidal arrangement of columns that, to the best of our knowledge, was not yet generated by any other methodology.

Results and discussion

Principles of self-organization of self-assembling dendrons, dendrimers, and dendronized polymers

The mechanisms of reversible transformation of supramolecular columns and spheres are summarized in Fig. 1. During the phase transition from supramolecular columns to supramolecular spheres observed upon heating, the electron density of the aligned columns is reorganized due to the intramolecular movement of the self-assembling molecules, producing the orientationally disordered supramolecular spheres (Fig. 1a). These supramolecular spheres look-like giant atoms but they differ fundamentally from atoms since they are highly dynamic structures with their components interchanging between spheres, columns and spheres and columns [35]. Recently, thermodynamically stable columns self-organized from spheres, including chiral, were discovered [57–59,66]. The rational of the stability of supramolecular columns self-organized from sphere was not yet elucidated. The spheres from Fig. 1 are in fact a simplified representation of polyhedral structures that were discussed as a function of molecular structure in a different publication [52]. For simplicity in this publication, they will be called spheres. It is also important at this point to mention that the 3D Frank-Kasper phases and the quasicrystals discussed here can be considered as 3D crystals or quasicrystals if we refer to the structure of the supramolecular spheres or liquid crystals if we refer to the structure of the dendrons or dendrimers forming the sphere. Regardless of their name these supramolecular spheres are dynamic allowing motion and interchange-rearrangements of their components. The process of this first order phase transition is reversible.

* Corresponding author.
E-mail address: percec@sas.upenn.edu (V. Percec).
Received 13 October 2021; Received in revised form 22 October 2021; Accepted 23 October 2021

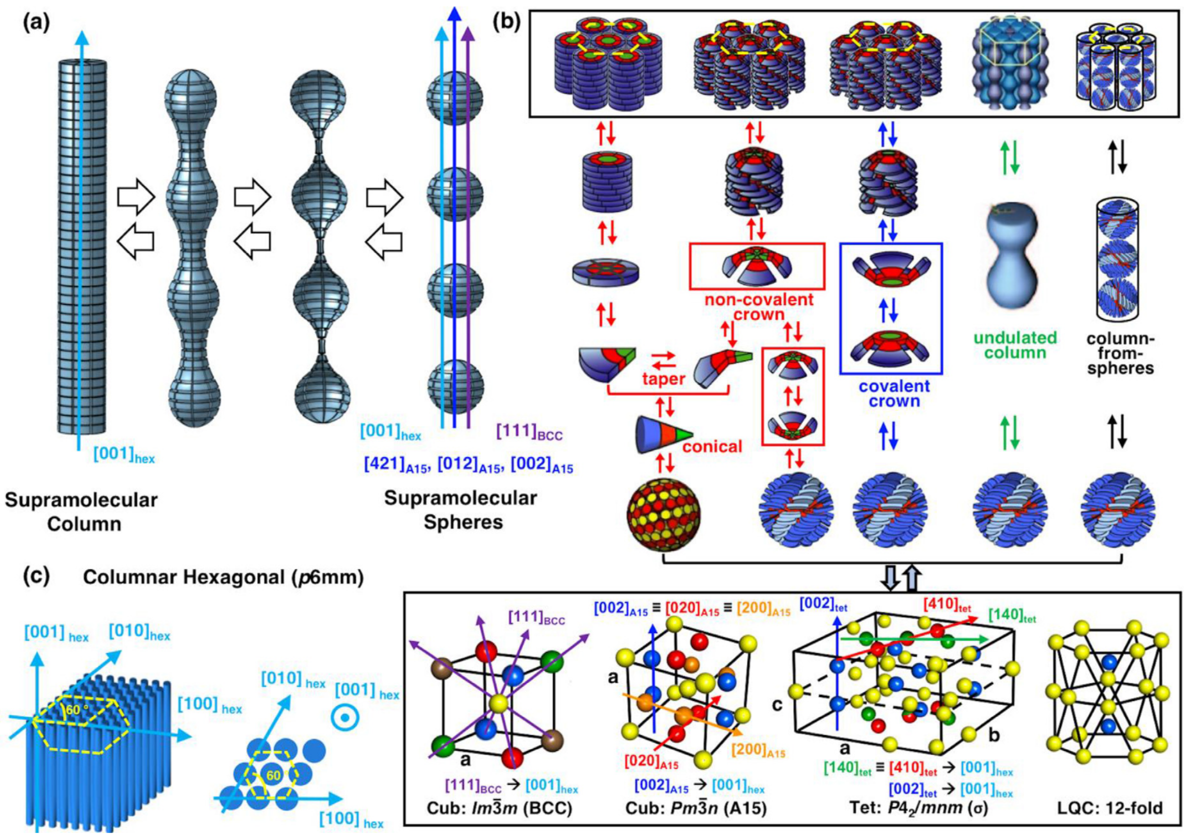

Fig. 1

(a) A simplified scheme of the reversible transformation between supramolecular columns and spheres when fragments of columns move to create regions of high and low electron density. The close contact directions of spheres in $Im\bar{3}m$ (BCC), $Pm\bar{3}n$ (A15 Frank-Kasper) phases that nucleate the long axis of the column are shown. (b) A more detailed molecular description of panel (a). Supramolecular hexagonal columns generated from tapers, crowns, undulated columns, or spheres transform into supramolecular columns. Columns generated from covalent crowns require the lowest number of steps and a concerted rather than stepwise process to transform into spheres [25,26]. Depending on the strength of the interaction at the apex, supramolecular non-covalent crown-based columns can follow both covalent crown-like or taper pathways. (c) Crystallographic directions in the columnar hexagonal, $Im\bar{3}m$ (BCC), $Pm\bar{3}n$ (A15 Frank-Kasper), $P4_2/mnm$ (σ Frank-Kasper) and liquid quasicrystal (LQC) periodic and quasiperiodic arrays. The close contact spheres in the BCC, A15 and σ are indicated with continuous colored lines.

Fig. 1b illustrates the hierarchical mechanisms of the reversible transformation between columnar and spherical phases, including BCC, A15, σ, and LQC. Supramolecular columnar hexagonal arrays self-assembled from tapered and conical dendrons [4,5,53,54], covalent crowns [22,23,55,56], non-covalent crowns [4,5,25,26], undulated columns [57,66], and columns-from-spheres [58,59] are illustrated. Comparison of the unit cells of the columnar and spherical phases is present in Fig. 1c with close contact spheres labeled in the same colors.

To date, four distinct SOM effects have been observed. They are summarized in Fig. 2 with the columnar hexagonal and cubic lattices shown in the left columns, the resulting architectures presented in the middle column and the chemical structures in the right columns. Orthogonal architectures of hexagonal columns have been obtained for a dendronized cyclotriveratrylene (Fig. 2a) [22] and a dendronized cyclotetraveratrylene [25] by the epitaxial nucleation of the columns along the close contact $[200]_{A15}$ direction of a $Pm\bar{3}n$ (Frank-Kasper A15) cubic phase (Fig. 2a) [22]. A tetrahedral architecture of hexagonal columns of a dendronized perylene bisimide was subsequently discovered upon cooling a body-centered cubic (BCC, *Im3m*) phase, where the epitaxial nucleation occurred along the close contact $[111]_{BCC}$ direction (Fig. 2b) [23,24]. Most recently, two alternative SOMs arising from *Pm3n* cubic phase were reported, in which alignment by epitaxial nucleation along the close contact $[210]_{A15}$ direction generated a distorted dodecahedral arrangement of hexagonal columns of a second generation dendron with a carboxylic acid at its apex (Fig. 2c) [25], while alignment along the close contact $[421]_{A15}$ direction of an amphiphilic Janus dendrimer produced rhombitruncated cuboctahedral helical columns (Fig. 2d) [26]. In all cases, the dendronized molecule exhibiting SOM could adopt either a covalent [22,23,25] or a supramolecular crown-like conformation that was recently proposed to be critical for SOM due to its fewer number of concerted rather than a larger number of stepwise steps in the process of self-organization that is required by conical self-assembling dendrons [25,26]. The results summarized in Fig. 2 indicate that covalent self-assembling crowns prefer to self-organize by SOM tetrahedral and orthogonal arrays that are generated by epitaxial nucleation *via* the close-contact spheres of their cubic phase. Supramolecular crowns may select alternative pathways during SOM. Currently the rational for the decission for this selection is not yet elucidated.

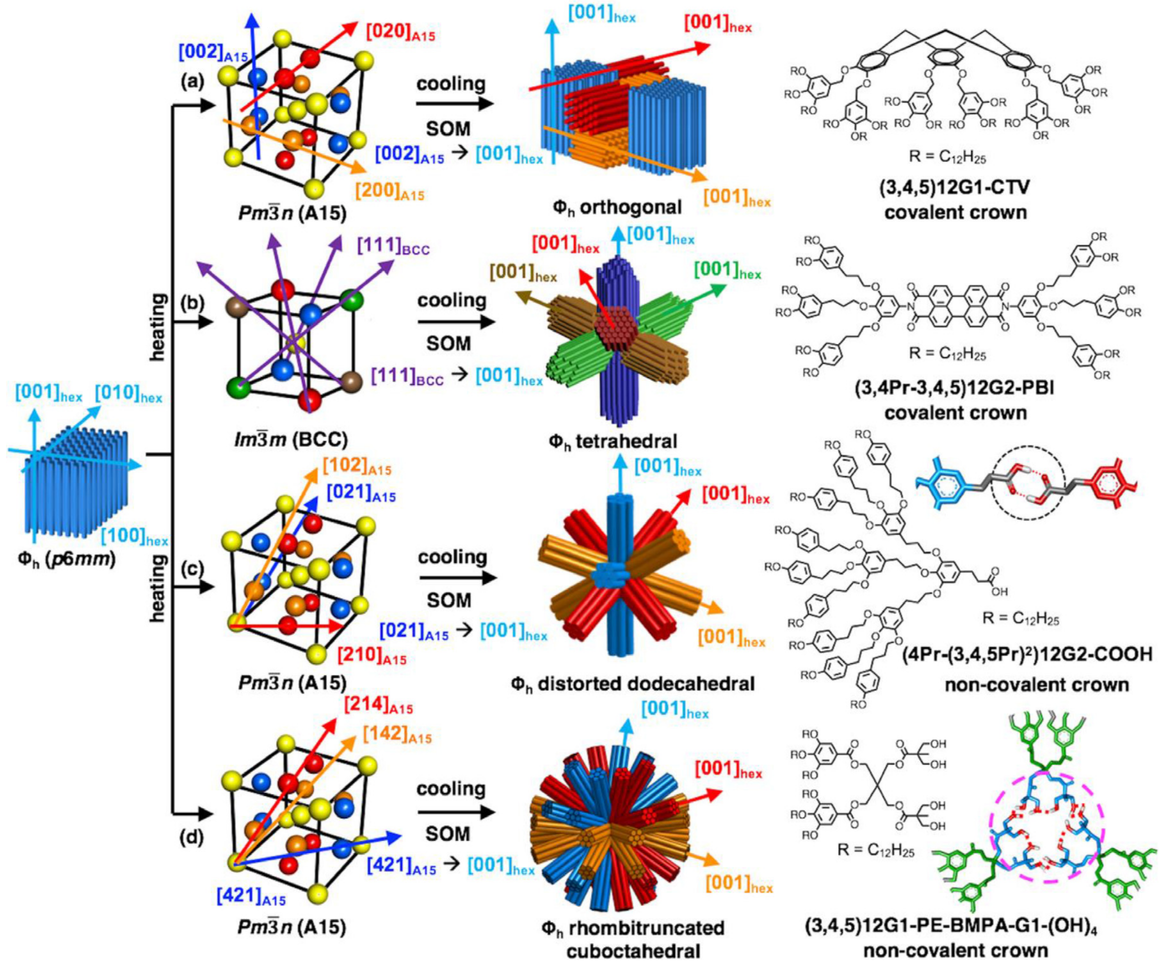

Fig. 2

Summary of already published SOMs generating new hexagonal arrangements of columns. (a) Orthogonal arrangement by following the close contact direction along $[200]_{A15} \rightarrow [001]_{hex}$ in $Pm\bar{3}n$ (A15). (b) Tetrahedral arrangement by following the close contact direction along $[111]_{BCC} \rightarrow [001]_{hex}$ in $Im\bar{3}m$ (BCC). (c) Distorted dodecahedral arrangement by following the close contact direction along $[210]_{A15} \rightarrow [001]_{hex}$ in $Pm\bar{3}n$ (A15). (d) Rhombitruncated cuboctahedral arrangement by following the close contact direction along $[421]_{A15} \rightarrow [001]_{hex}$ in $Pm\bar{3}n$ (A15). Covalent crowns are forming columns and spheres in (a) and (b) while a supramolecular H-bonding crown-assembled columns and spheres in (c) and (d).

However, more experiments are epected to provide a moleculkar engineering approach of new morphjologies *via* SOM.

Synthesis of the dendronized triphenylene (3,4,5)12G1-Tp

After we searched for candidate molecules which showed a phase transition from a hexagonal phase to a tetragonal phase, the dendronized triphenylene (Tp) with six 3,4,5-tris(dodecyloxy)benzyl ethers on its periphery, (3,4,5)12G1-Tp (Figs. 3 and S1), was selected. Tp is a classical disk-like molecule which can be synthesized *via* Scholl trimerization [123] of veratrole. Dendronized Tp was demonstrated to form crown-like architectures which self-assembled into helical columns and spheres. (3,4,5)12G1-Tp was synthesized again by a procedure reported previously from our laboratory [55] and purified until the melting transitions did not change and remained constant. This very high level of purity is demanded by the SOM process. A combination of techniques that includes thin-layer chromatography (TLC), high-pressure liquid chromatography (HPLC), ^{1}H and ^{13}C NMR, and matrix-assisted laser desorption/ionization time-of-flight mass (MALDI-TOF) spectrometry were employed to analyze the structures and to assess the higher than 99% purity of the intermediary (Figs. S2–S5) and final compounds (Figs. S6–S9). Due to additional numbers of column chromatography purifications and precipitations compared to the previous publication [55], the target dendrimer molecule showed higher phase transition temperatures including higher melting point (from 100 °C to 108 °C), and sharper phase transitions by DSC. They will to be discussed later.

Preparation of oriented fibers for XRD analysis

Aligned fibers were prepared according to a procedure elaborated in our laboratory by using the extrusion device shown in Fig. S10 [60] in the Supplemental Information.

Thermal and structural characterization of dendronized triphenylene (3,4,5)12G1-Tp by DSC and XRD

Dendronized triphenylenes self-assemble into supramolecular helical columns and spheres *via* their crown conformation [55],

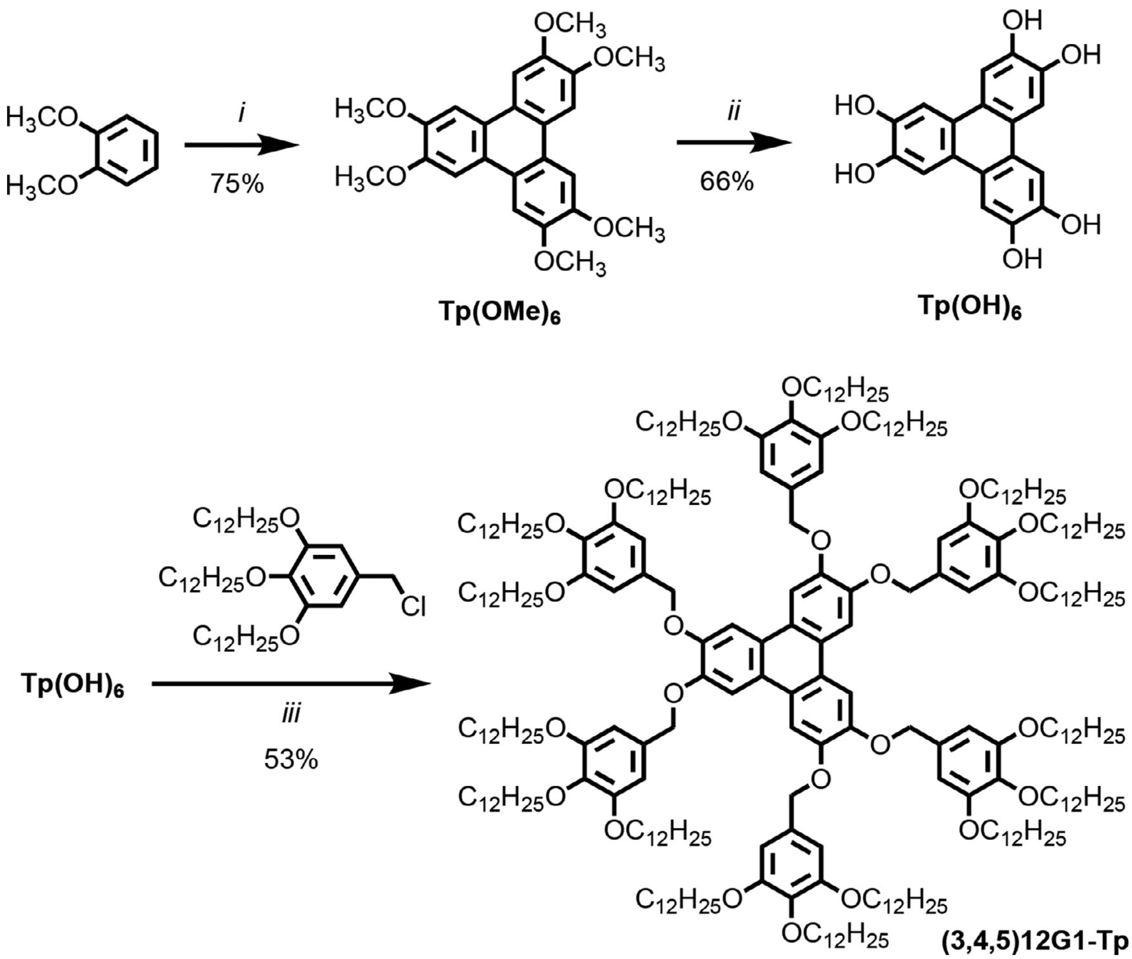

Fig. 3

Synthesis of dendronized triphenylene (3,4,5)12G1-Tp. Reagents and Conditions: (i) $FeCl_3$, H_2SO_4(conc.), CH_2Cl_2, 23 °C, 3 h; (ii) HBr (48% in H_2O), AcOH, 130 °C, 12 h; (iii) K_2CO_3, DMF-THF (2:1), 70 °C, 24 h.

which was suggested to be the secondary structure required for SOM since it undergoes the reversible sphere-column transition in a fewer number of concerted steps rather than a process containing a larger number of stepwise events [22]. SOM also demands a transition between a columnar hexagonal array (Φ_h) and a lattice generated from supramolecular spheres. (3,4,5)12G1-Tp (Fig. 4a) is the simplest dendronized triphenylene that exhibits such a phase transition, specifically between a helical columnar hexagonal phase with intracolumnar order (Φ_h^{io}) and a tetragonal $P4_2/mnm$ periodic array (Fig. 4b) demonstrated previously by powder XRD in 2009 [55]. The 2009 publication [55] was published before the discovery of the first example of SOM by fiber XRD in 2016 [22]. The structures of the Φ_h^{io}, and tetragonal $P4_2/mnm$ phases, denoted hereafter as Tet or Frank-Kasper σ, will be discussed later in more details. Thermal analysis of (3,4,5)12G1-Tp by differential scanning calorimetry (DSC) indicates that (3,4,5)12G1-Tp self-organizes into multiple lattices (Fig. 4c, Table S1 and S2). Upon heating at 10 °C/min, (3,4,5)12G1-Tp transitions at 8 °C from a crystalline columnar hexagonal (Φ_h^k) 3D array to a 2D Φ_h^{io} helical columnar hexagonal phase with intracolumnar order. Helical ϕ_h^{io} transitions to the $P4_2$/mnm (σ) phase at 42 °C upon heating and re-forms upon cooling from the $P4_2$/mnm (σ) phase at 10 °C/min to below 26 °C. Heating the $P4_2$/mnm (σ) phase above 96 °C generates a Pm3n cubic phase, known also as the Frank-Kasper A15 phase. The Pm3n cubic phase melts to an isotropic liquid at 108 °C. The structure of all phases was assigned using XRD analysis (Table S2) [55].

Small-angle X-ray diffractograms of the aligned fiber of (3,4,5)12G1-Tp are presented in Fig. 4d–g. Initial XRD structural analysis was performed using Datasqueeze (version 3.0.5) [124]. XRD at 23 °C (Fig. 4d, h) is consistent with a helical Φ_h^{io} array with column diameter, $D_{col} = a$, of 35.4 Å (Table S2). The equatorial position of the $(100)_{hex}$ reflection indicates that the column axis of the Φ_h^{io} array, $[001]_{hex}$, is aligned along the fiber axis (Fig. 4d). The oriented fiber XRD patten of the Φ_h^{io} at 23 °C (Fig. 4d) with additional off-axis features is resembling the pattern of the oriented fibers obtained from supramolecular columns in a ϕ_h phase self-organized from spheres including chiral spheres [58,59], and from undulated columns [57,66]. The additional XRD feature of the columns from Fig. 4d is their helical character that is most clearly observed in Fig. 4f. The helicity of these columns was best observed by a combination of fiber XRD and circular dichroism experiments after their complexation with chiral electron acceptor compounds [55]. The wide-angle X-

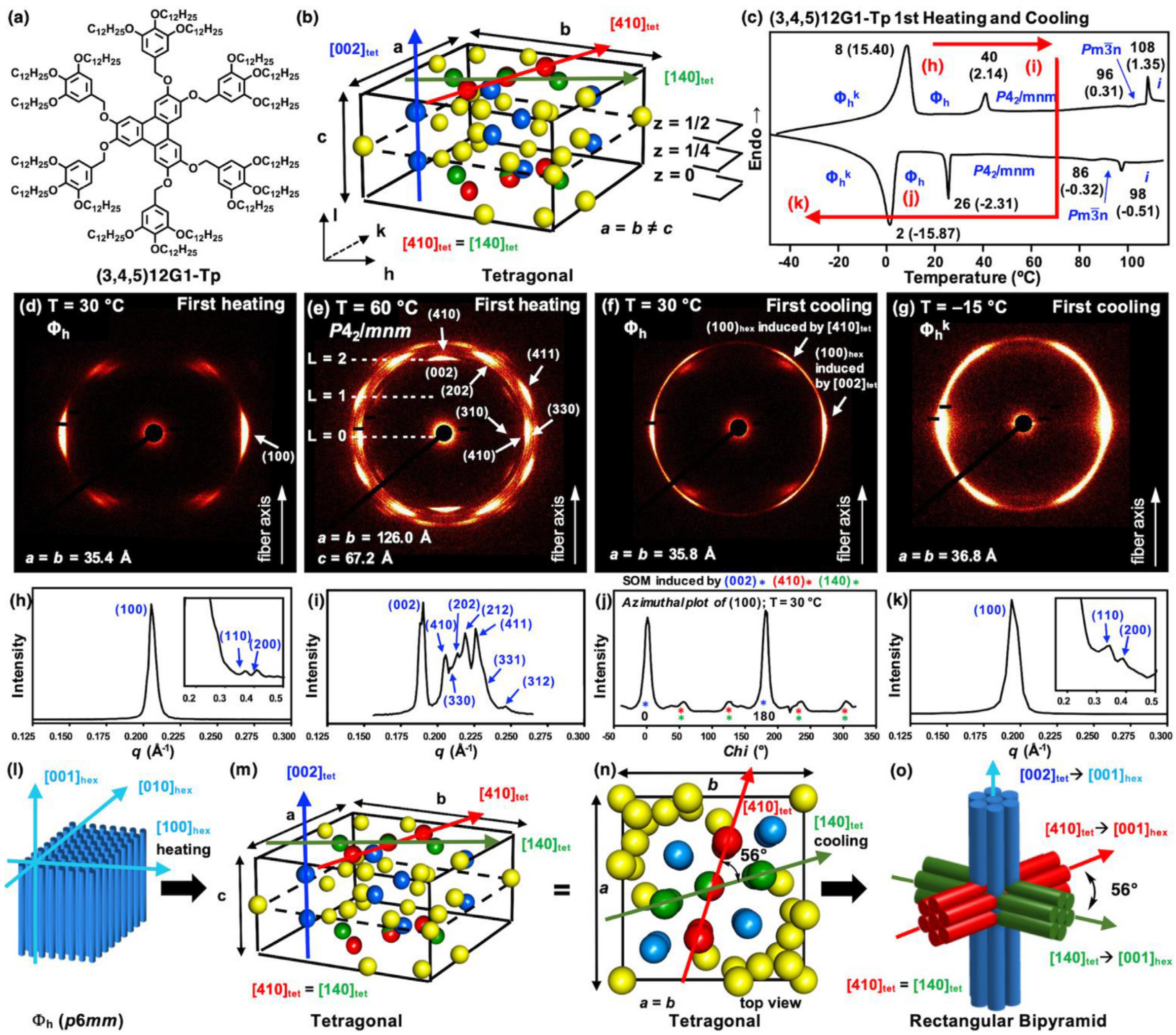

Fig. 4

Structural analysis of supramolecular assemblies generated by SOM from (3,4,5)12G1-Tp. (a) Structure of (3,4,5)12G1-Tp. (b) Unit cell of $P4_2/mnm$ (σ) lattice. Spheres in close contact along the indicated directions are colored alike and are linked by blue, red and green lines. The yellow spheres follow the spheres of the red, green and blue arrows by a mechanism not yet known. (c) DSC traces of first heating and cooling scans of (3,4,5)12G1-Tp at 10 °C/min. Phases indexed by XRD, transition temperatures (in °C), and associated enthalpy changes (in parentheses in kcal/mol) are shown. (d–g) XRD of an aligned fiber obtained by extrusion at 23 °C of (3,4,5)12G1-Tp during first heating and cooling. Temperature and lattice parameters are indicated. (h, i, k) XRD diffractogram with expansions in inset panels. (*hkl*) indices are marked. (j) Azimuthal plot of $(100)_{hex}$ at 23 °C on cooling. (l–o) Schematic representation of the lattice transition between Φ_h and $P4_2/mnm$ on first heating and cooling. SOM induced by $[002]_{tet}$ and $[410]_{tet}$ to $[001]_{hex}$ results in a rectangular bipyramidal arrangement of columnar hexagonal domains. As shown in panel n and l the angle between [410] (red) and [140] (green) directions is ∼56° (For interpretation of the references to color in this figure legend, the reader is referred to the web version of this article.).

ray scattering (WAXS) data in the Φ_h^{io} phase (Fig. S11) showed clear features from the intermolecular distance (4.4 Å) along the fiber axis. It also supports that the supramolecular helical columns are aligned along the fiber axis direction. Upon heating to 60 °C, the Φ_h^{io} 2D lattice is transformed into the $P4_2/mnm$ (σ) phase (Fig. 4e, i). Indexing of the XRD data recorded at 60 °C is consistent with the $P4_2/mnm$ (σ) phase (Fig. 4e), with lattice parameters ($a = b = 126.0$ Å, $c = 67.2$ Å) in good agreement with those reported previously with a different X-ray machine ($a = b = 124.0$ Å, $c = 64.8$ Å) [55]. The equatorial position of peaks is consistent with $(hk0)_{tet}$ reflections, and the meridional position of $(002)_{tet}$, shows that the *c*-axis of the $P4_2/mnm$ (σ) unit cell is aligned with the fiber axis. Weak meridional $(410)_{tet}$ features along with off-axis $(002)_{tet}$ features (Fig. 4e) suggest that, upon heating, some $P4_2/mnm$ (σ) domains form such that $[410]_{tet}$ is aligned along $[001]_{hex}$. However, the weak intensity of off-axis $(002)_{tet}$ features indicate that the vast majority of $P4_2/mnm$ (σ) domains are arranged with $[002]_{tet}$ aligned along the preceding $[001]_{hex}$ direction (Fig. 4e). Therefore, heating from Φ_h^{io} to $P4_2/mnm$ (σ) does not erase the orientation of the sample (Fig. 3d) upon heating. The supramolecular sphere in $P4_2/mnm$ (σ) phase ($D_{sph} = 2(abc/40\pi)^{1/3} = 40.8$ Å) [53,55,62,71,72] was estimated to have a diameter close to that of the diameter of the supramolecular columns, D_{col}, that is 35.4 Å (Table S2). We employed this method for the calculation of the diameter of the supramolecular sphere in $P4_2/mnm$ (σ) lattice to be consistent with data reported previously

[53,55,62,71,72]. Cooling the aligned $P4_2/mnm$ (σ) phase from 60 °C to 23 °C, the Φ_h^{io} phase re-forms (Fig. 4f). However, four additional sharp (100) features appear in the X-ray diffractogram of the Φ_h^{io} phase obtained upon cooling from $P4_2/mnm$ (σ) (Fig. 4f) compared to the XRD recorded for Φ_h^{io} upon first heating (Fig. 4d). These features are consistent with directions of the $(100)_{hex}$ reflection that result from Φ_h^{io} phase where the column axes $[001]_{hex}$ are no longer aligned with the fiber axis [22–26]. An azimuthal plot of $(100)_{hex}$ shows that the additional four features that appear upon cooling occur 56° either side of the original $(100)_{hex}$ features (Fig. 4j). As will be shown more detail later, this azimuthal distribution is consistent with a Φ_h^{io} array with its column axis, $[001]_{hex}$, aligned along the $[410]_{tet}$ and the equivalent $[140]_{tet}$ directions of the preceding $P4_2/mnm$ (σ) phase (Fig. 4e). Further cooling the sample to –15 °C to the crystalline Φ_h^k phase, the similar off-axis $(100)_{hex}$ features were maintained (Fig. 4g, and k) as observed in the Φ_h^{io} phase at 23 °C upon cooling (Fig. 4f and j). Therefore, the XRD data in Figs. 4d and e provide evidence for SOM occurring in assemblies of (3,4,5)12G1-Tp, as summarized in Fig. 4l to o. The initial Φ_h^{io} array is aligned such that the supramolecular column axis, $[001]_{hex}$, is aligned along the macroscopic fiber axis. Upon heating from Φ_h^{io} to $P4_2/mnm$ (σ), the $[001]_{hex}$ directs the orientation of $[002]_{tet}$ so that the *c*-axis of the $P4_2/mnm$ (σ) lattice is aligned along the fiber axis. On cooling, domains of helical columns are formed not only along their original direction ($[002]_{tet} \rightarrow [001]_{hex}$), but also along two new directions: $[410]_{tet}$ and $[140]_{tet}$. As in previous SOM systems [22–26], we propose that the columns are packed into Φ_h^{io} domains, where $[001]_{hex}$ within each domain is induced by an epitaxial nucleation by a crystallographic direction from the preceding 3D phase generated from spheres. For (3,4,5)12G1-Tp, columnar domains are epitaxially nucleated along the $[002]_{tet}$, $[410]_{tet}$, and $[140]_{tet}$ directions of the preceding $P4_2/mnm$ (σ) phase, resulting in a rectangular bipyramidal arrangement of helical columns (Fig. 4o) that was observed for the first time in this study. When the second heating-cooling cycle was performed (Fig. 5), the azimuthal distribution in Φ_h^{io} phase (Fig. 5f) generated by SOM was maintained but became slightly diffuse. This indicated that the SOM reported here is reversible after this number of heating and cooling cycles. However, additional research is required to estimate stability after a larger number of heating-cooling cycles. Furthermore, the transition from $Pm\overline{3}n$ cubic (A15) to $P4_2/mnm$ tetragonal (σ) phase and then to Φ_h^{io} phase by aligned fiber of (3,4,5)12G1-Tp which generates another more complicated SOM will be reported in a different publication.

Analysis of the phase transitions of dendronized triphenylene (3,4,5)12G1-Tp by solid-state ^{1}H NMR

To understand the phase transitions of the extruded aligned fiber of the dendronized triphenylene (3,4,5)12G1-Tp, solid state NMR was utilized as a complementary method to DSC and XRD [42,55] on the same aligned fibers as the one employed for X-ray experiments. In the cubic phase at 100 °C, ^{1}H magic angle spinning (MAS) NMR spectra recorded on aligned fiber showed well resolved peaks like in the isotropic melt (Fig. 6) and in solution (Fig. S6).

This demonstrates high mobility for the dendronized Tp in self-organized state. In $P4_2/mnm$ (σ) phase in the rage from 80 to 50 °C, the signals from the aromatic protons *a* and *b* merged into a broad peak (Fig. 6, red circle), and the signal of the benzyl proton *c* almost disappeared. The splitting of the signals in the isotropic phase and cubic phase between *d* and *d′* or *e* and *e′* result from local differences of the dodecyloxy side chains attached in *meta* or *para* position to the outer phenyl rings. In contrast, the splitting of the methyl signal *o, o′* observed exclusively in the $P4_2/mnm$ (σ) phase (Fig. 6, green circle) originates from local packing density differences of the methyl groups and vanishes upon going to more symmetric lattices in $Pm\overline{3}n$ cubic (A15) high temperature phase, and in the lower temperature Φ_h^{io} phase. The solid-state NMR obtained here with extruded oriented fiber sample showed higher resolution compared with our previous publication [55] used to confirm the phase transitions of (3,4,5)12G1-Tp.

Supramolecular spheres in the $P4_2/mnm$ *(Frank-Kasper σ) tetragonal phase*

To understand the mechanism by which SOM occurs between $P4_2/mnm$ (σ) and ϕ_h^{io} phases, it is necessary to briefly discuss the supramolecular spheres that generate the unit cell of the $P4_2/mnm$ (σ) tetragonal phase (Fig. 4b) [28]. The $P4_2/mnm$ (σ) unit cell contains 30 spheres. The average number of molecules per supramolecular sphere was determined to be 4.9 ($\mu = (abc\rho N_A)/(MW \times 30)$). This number was calculated with the lattice parameter (*a, b, c*), the molecular weight of the dendron (MW), the experimental density ($\rho = 0.951$ g/cm^3), and Avogadro's number (N_A) (Table S2). Therefore, each sphere of the $P4_2/mnm$ (σ) tetragonal lattice consists of five covalent crown-like molecules. As is typical for Frank-Kasper phases [61], the $P4_2/mnm$ (σ) unit cell contains alternating planes of densely- and sparsely packed spheres (Figs. 4b and 7). Planes at $z = 0$ and ½ feature 11 spheres each, depicted in yellow, red, and green in Figs. 4b, 7b, and 7d. Spheres colored in red and green are separated by $0.259a = \frac{\sqrt{2}}{2(1+\sqrt{3})}a = 32.6$ Å (Fig. S12). These distances suggest that the spheres, which have a diameter of 40.8 Å (Table S2), are in close contact, along the equivalent $[410]_{tet}$ and $[140]_{tet}$ directions, respectively. It should be noted that calculation of the diameter of the supramolecular sphere ($D_{sph} = 2(abc/40\pi)^{1/3} = 40.8$ Å) [53,55,62,71,72] assumes that the entire volume of the unit cell is divided between 30 ideal spheres of identical volume, without considering the polygonal shape of objects in the lattice [47] and any available void space, while the close contact distances (32.6 Å) (Fig. S12) should not surprise that is as expected smaller than to the diameter of supramolecular spheres (40.8 Å). In fact the smaller value of the distance between the centers of spheres than that of the sphere diameter provides a very strong support for the polygonal shape of "spheres." However, the sphere is a simplified model of polyhedral objects [47,52,53,55,62,71,72], and therefore, the calculated diameter (40.8 Å) should be slightly larger than the close contact distance between then polygonal "spheres" (32.6 Å). These close contacts are not continuous between unit cells (Fig. 7b, c). In contrast, planes at z = ¼ and ¾ are sparsely populated by only 4 spheres (depicted in blue in Fig. 7a and d), separated in the $[002]_{tet}$ direction by 0.5 c (= 33.6 Å). These blue spheres

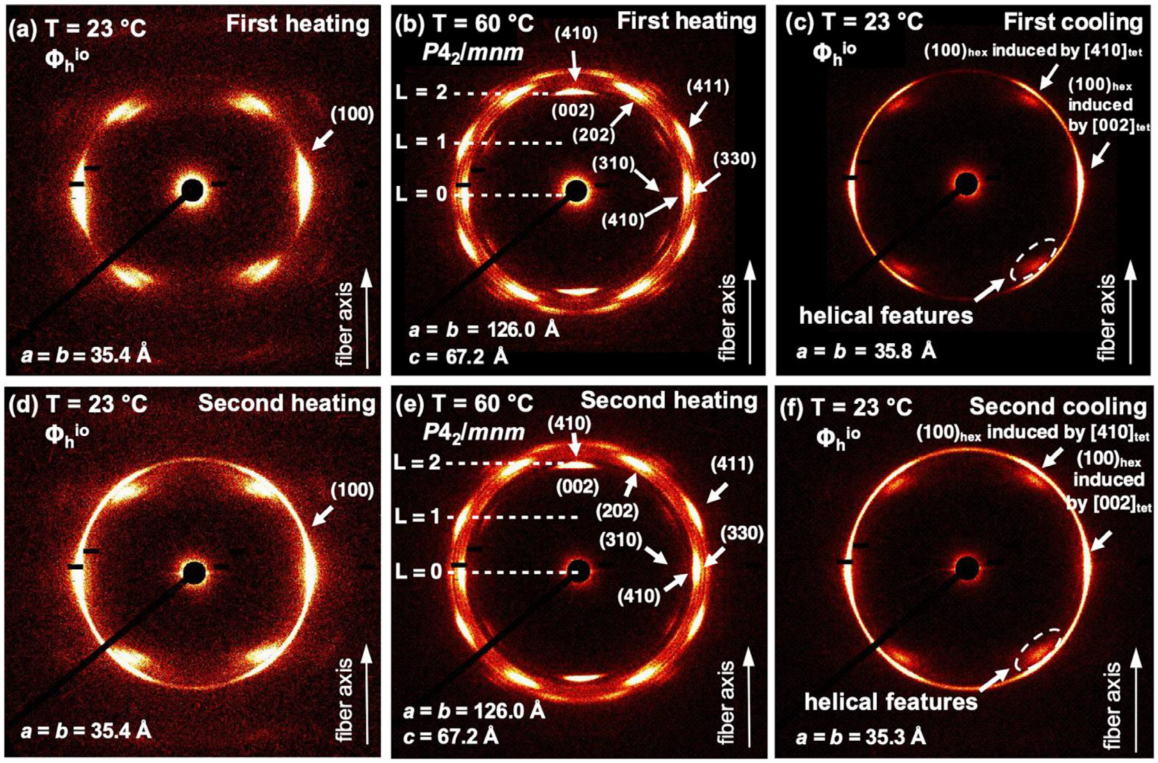

Fig. 5

Experimental SAXS patterns of the Φ_h^{io} and $P4_2/mnm$ (σ) phases collected from an aligned fiber upon (a, b) first heating, (c) first cooling, (d, e) second heating, and (f) second cooling. Temperature, fiber axes, phases, heating and cooling cycles and unit cell parameters are indicated.

are therefore, in close contact continuously along $[002]_{tet}$ across multiple unit cells (Fig. 7a).

Epitaxial nucleation transforming supramolecular spheres along $[002]_{tet}$ into helical columns along $[001]_{hex}$

The relative intensities of the $(100)_{hex}$ features in the fiber XRD of Φ_h after cooling from the $P4_2/mnm$ (σ) phase (Fig. 4e, i) suggest that the majority of columns recover their alignment along the macroscopic fiber axis. This implies that the majority of unit cells in the $P4_2/mnm$ (σ) phase generate helical columnar hexagonal domains where the emergent $[001]_{hex}$ is aligned along the $[002]_{tet}$ direction.

The close contact between the blue spheres along the $[002]_{tet}$ direction is not disrupted during the transition from $P4_2/mnm$ (σ) to Φ_h^{io} (Fig. 8a). This provides a low barrier to the conversion of discrete spheres into continuous supramolecular columns and therefore, this direction is responsible for the epitaxial nucleation. This process favors the translation of other spheres within the $P4_2/mnm$ (σ) unit cell to form a hexagonal array of $[002]_{tet}$-aligned columns by epitaxial nucleation and growth.

Epitaxial nucleation transforming supramolecular spheres along $[410]_{tet}$ to helical columns along $[001]_{hex}$

The four distinctive off-equator peaks of the $(100)_{hex}$ features in the fiber XRD of Φ_h^{io} after cooling from the $P4_2/mnm$ (σ) phase (Fig. 4e, i) suggest that a fraction of helical columns nucleate their alignment along the $[410]_{tet}$ and the equivalent $[140]_{tet}$ directions. The close contacts between the red spheres along the $[410]_{tet}$ direction and the green spheres along the $[140]_{tet}$ directions are not continuous throughout a domain of unit cells during the transition from $P4_2/mnm$ (σ) to Φ_h^{io} (Fig. 8b, c). Therefore, rearrangements dictated by the column formation along the $[410]_{tet}$ and $[140]_{tet}$ directions are necessary, leading to a higher barrier to the conversion of discrete spheres into columns when compared with the $[002]_{tet}$ direction. The resulting column axes induced by $[410]_{tet}$ and $[140]_{tet}$ upon cooling are perpendicular to the axis of the aligned fiber, generating a rectangular bipyramidal arrangement of columnar hexagonal domains.

Structural and retrostructural analysis of xrd experiments performed on oriented fibers indicate self-organization of rectangular bipyramidal arrangements of helical columnar hexagonal domains

The theoretical XRD pattern of the rectangular bipyramidal arrangement of columnar hexagonal domains (Fig. 9a) includes diffraction features arising from the $[002]_{tet}$-aligned columns (Fig. 9b) and those arising from the $[410]_{tet}$-aligned columns (Fig. 9c). The XRD pattern of the $[002]_{tet}$-aligned columns corresponds to the strong $(100)_{hex}$ peaks on the equator, that are perpendicular to the fiber axis. XRD pattern of the $[410]_{tet}$-aligned columns correspond to six distinctive off-equator $(100)_{hex}$ peaks, resulted from the hexagonal pattern of the columns. The superposition of these features produces a theoretical XRD pattern that is consistent with the experimental XRD of (3,4,5)12G1-Tp in the Φ_h^{io} phase (Fig. 9d).

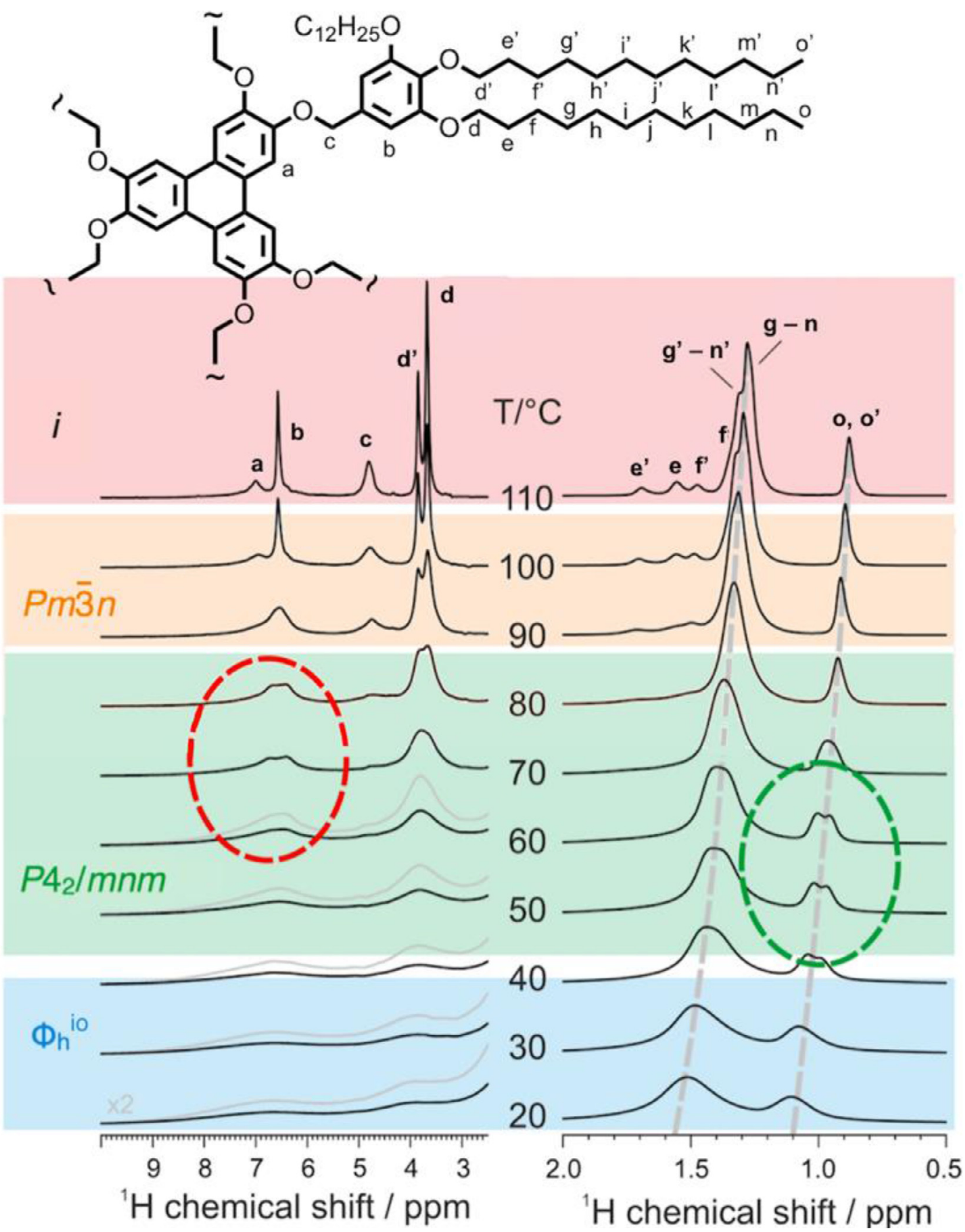

Fig. 6

Variable temperature ^{1}H MAS NMR spectra of (3,4,5)12G1-Tp recorded on heating of an annealed oriented fiber sample prepared by extrusion at 25 kHz MAS spinning frequency and 700 MHz ^{1}H Larmor frequency. The splitting of the signals in the isotropic phase at 110 °C between *d* and *d'* or e and *e'* result from local differences of the $OC_{12}H_{25}$ side chains attached in meta or para position to the outer phenyl rings. In contrast, the splitting of the methyl signal o, o' in the $P4_2/mnm$ (σ) phase originates from local packing differences of the methyl groups and vanishes upon going to higher temperature and more symmetric lattice (For interpretation of the references to color in this figure, the reader is referred to the web version of this article.).

While the rectangular bipyramidal arrangement of helical columnar hexagonal domains illustrated in Fig. 9 represents a new supramolecular arrangement of helical columns, this architectural motif raises more new fundamental questions that must be elucidated than the single question answered. Some of these questions are determined by the ratio between the rates of epitaxial nucleation versus helical columnar hexagonal growth. If nucleation is rare or slow and growth relatively fast, the columnar new phase nucleated epitaxially dominates the entire volume. Conversely, if nucleation is easy or fast and frequent in the bulk of the sample, the resulting columns would be oriented randomly. The results from Fig. 5 may indicate a relatively slow nucleation and a fast growth. However, a large diversity of experiments is required to confirm this hypothesis. If nucleation is slow and

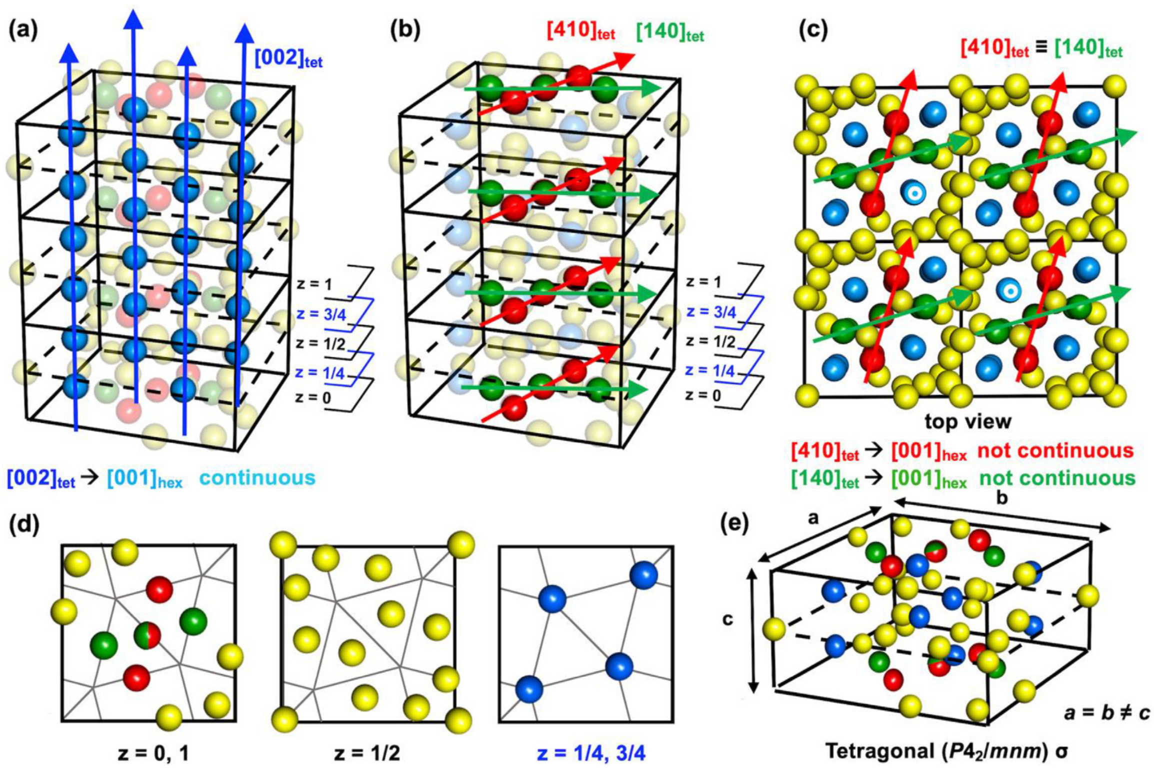

Fig. 7

Arrangement of supramolecular spheres in $P4_2/mnm$ (σ) phase. (a) Blue spheres exhibit close contact along the $[002]_{tet}$ direction at a distance of 0.5 c (= 33.6 Å). (b) Red and green spheres exhibit close contact along the equivalent $[410]_{tet}$ and $[140]_{tet}$ directions at a distance of 0.259 a (= 32.6 Å). (c) Close contact directions between supramolecular spheres along $[410]_{tet}$ and $[140]_{tet}$ are not continuous between unit cells. (d) Supramolecular spheres on crystal planes with $z = 0$, ¼, ½, ¾, and 1. (e) Unit cell of $P4_2/mnm$ (σ) with spheres colored. Diameter of a supramolecular sphere is approximately 40.8 Å ($D_{sph} = 2(abc/40\pi)^{1/3}$ [53,55,62,71,72]. During the epitaxial nucleation process the yellow spheres that are as closed to each other as the red or green spheres will follow the direction of the blue, red and green arrows that indicate the largest number of close contact spheres on one arrow (For interpretation of the references to color in this figure legend, the reader is referred to the web version of this article.).

columnar growth is fast the first question to ask is how do the rectangular bipyramidal arrangements of helical columns pack together? Fig. 9 illustrates only one such architectural motif, but it does not indicate how a large density of this architectural motif will self-organize or disorganize the original periodic arrays. The extensive experience in our laboratory with the design of self-assembling crown-like dendrons and dendrimers indicates that we will be able to design SOM effects at the transition between any sphere forming periodic or quasiperiodic arrays containing close contact spheres and columnar hexagonal or even other columnar lattices. We may ultimately be able to even engineer the resulting architectural motif by being able to predict the direction of the epitaxial nucleation mediated by the largest number of close contact spheres on one director. However, the largest challenge remains that of the detailed structural analysis of the resulting self-organization. So far this was performed only for the orthogonal arrangement of columns, to a certain extent, by determining the detailed structure of the oriented domains by polarized birefringence microscopy combined with oriented fiber XRD experiments [22].

Conclusions

A new SOM has been demonstrated for the nanoscale periodic arrays of (3,4,5)12G1-Tp. Supramolecular helical columns with preferential alignment within a Φ_h^{io} array generate, upon heating, a $P4_2/mnm$ (σ) tetragonal phase with preferred alignment. Upon cooling, the crystallographic directions of $P4_2/mnm$ (σ) lattice generate a complex rectangular bipyramidal arrangement of columnar hexagonal domains, oriented by an epitaxial nucleation along the $[002]_{tet}$ and $[410]_{tet}$ directions. Structural analysis using oriented fiber XRD experiments confirms this transformation along the $[002]_{tet}$ and the $[410]_{tet}$ directions, which involves the transition of supramolecular spheres into helical columns while preserving their close contact directions that are determined by the largest number of close contact spheres on one direction.

The resulting rectangular bipyramidal architecture of helical columns arranged in a hexagonal array was not yet generated by any other methodology and represents the first example of SOM effect mediated by a non-cubic phase. By analogy with generational libraries of self-assembling dendrons [4,5,53], a collection of SOM libraries is emerging (Fig. 10). Together with SOMs reported previously (Figs. 2 and 10), the results presented here support the proposal that SOM is epitaxially nucleated by spheres formed from crown-like conformers, rather than spheres assembled from conical molecules (Fig. 1b) [25]. These findings raise many questions: can SOM be generalized from all Frank-Kasper and related phases such as LQC generated

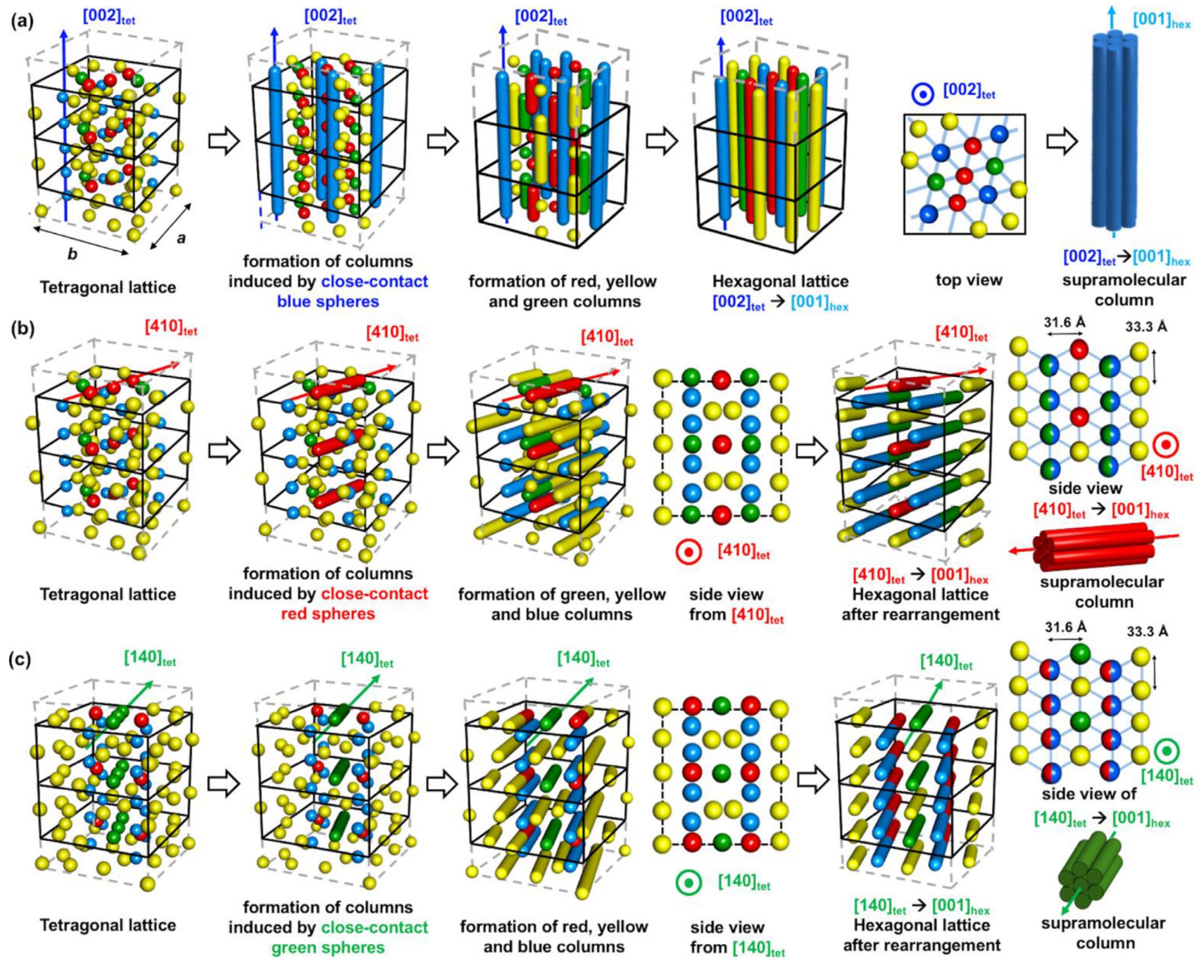

Fig. 8

Mechanism proposed for sphere to column transition mediated by epitaxial nucleation (a) $[002]_{tet} \rightarrow [001]_{hex}$, (b) $[410]_{tet} \rightarrow [001]_{hex}$ and (c) $[140]_{tet} \rightarrow [001]_{hex}$. Close contact spheres along (a) blue spheres along $[002]_{tet}$, (b) red spheres along $[410]_{tet}$ and (c) green spheres along $[140]_{tet}$ form columns upon cooling by merging with other colored spheres including the yellow spheres following the close contact direction of epitaxial nucleation. For simplicity in panels a, b and c four different colored spheres are forming four different colored columns that follow only one of the three colored directions showed in the right column of the figure. Transformation of spheres to columns provides a hexagonal lattice in which $[002]_{tet,}$ $[410]_{tet}$ or $[140]_{tet}$ directions have been preserved as $[001]_{hex}$ column axis (For interpretation of the references to color in this figure legend, the reader is referred to the web version of this article.).

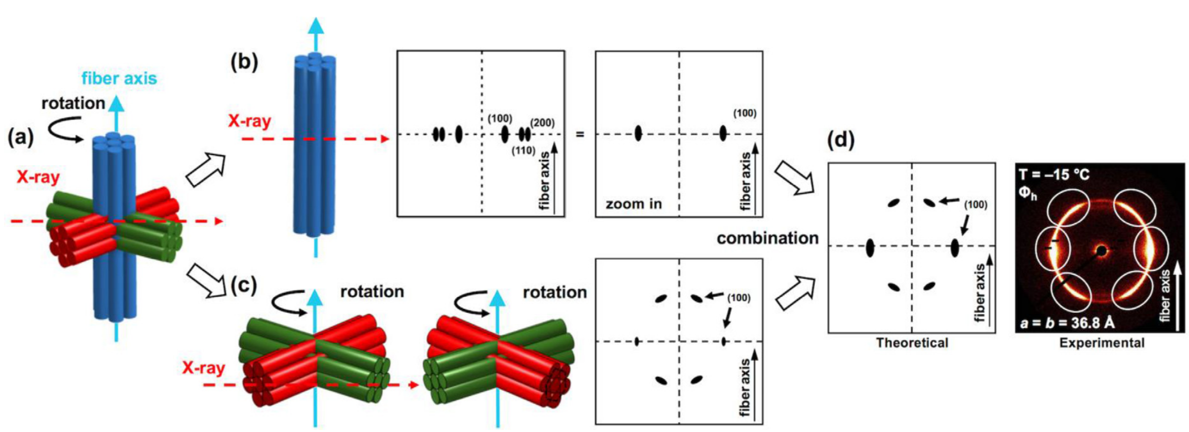

Fig. 9

Analysis of XRD experiments of oriented fibers. (a) Schematic of columnar hexagonal domains epitaxially nucleated along the $[002]_{tet}$ (blue) and $[410]_{tet}$ (red and green) close contact directions. (b) Theoretical XRD patterns from columns nucleated along $[002]_{tet}$. (c) Theoretical XRD patterns nucleated from columns along $[410]_{tet}$ and $[140]_{tet}$. (d) Comparison of (left) the final theoretical XRD pattern combined from (b, c) and (right) the experimental XRD pattern of (3,4,5)12G1-Tp after cooling from the $P4_2/mnm$ (σ) phase (For interpretation of the references to color in this figure legend, the reader is referred to the web version of this article.).

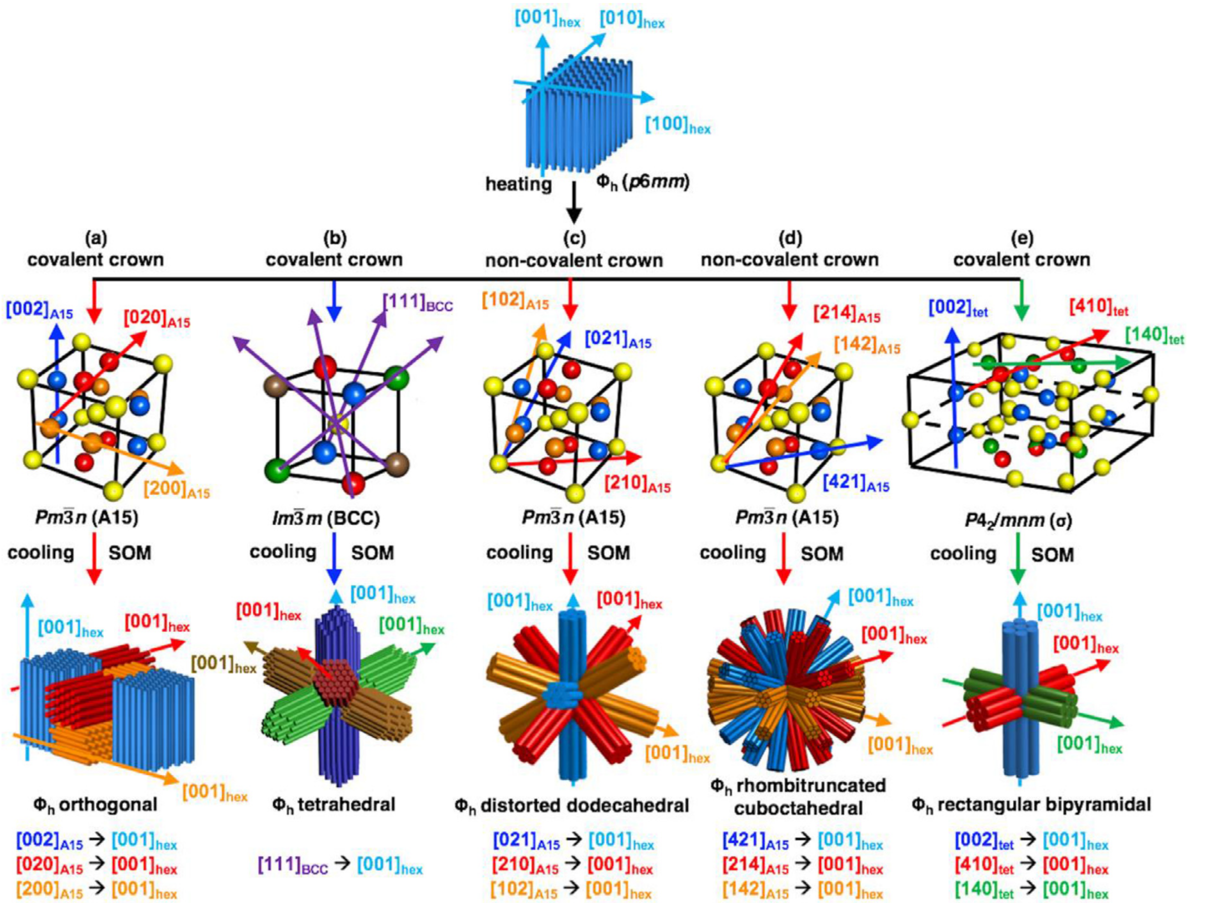

Fig. 10

Summary of the five columnar hexagonal nanoscale arrangements mediated by SOM. Previous SOMs have generated (a) an orthogonal arrangement of hexagonal columns from covalent crown-assembled spheres along $[200]_{A15} \rightarrow [001]_{hex}$. (b) Tetrahedral arrangement of hexagonal columns from covalent crown-assembled spheres along $[111]_{BCC} \rightarrow [001]_{hex}$. (c) Distorted dodecahedral arrangement of hexagonal columnar from supramolecular H-bonding crown-assembled spheres along $[210]_{A15} \rightarrow [001]_{hex}$. (d) Rhombitruncated cuboctahedral arrangement of hexagonal columnar from supramolecular H-bonding crown-assembled spheres along $[421]_{A15} \rightarrow [001]_{hex}$. In this report, (e) the new rectangular bipyramidal arrangement of helical columnar hexagonal domains is generated by cooling a $P4_2/mnm$ (σ) phase to a columnar hexagonal phase.

from spheres, assembled not only from crown-like molecules but also from conical molecules forming micellar spheres? Can this SOM process be also applied to other helical columnar hexagonal architectures such as cogwheel [79–81] and hat-shaped [82] derived supramolecular polymers, and even from self-organizable dendronized covalent polymers that exhibit crown conformations [29,30,72,83,84]? Are the close contact interactions between spheres within periodic arrays of other forms of soft matter such as block copolymers, giant molecules, and surfactant able to exhibit SOM? How can the interplay between the translation of supramolecular objects and the close contact spheres or continuous columnar character be designed to favor one SOM effect over another? Answering these questions will continue to develop SOM as a general methodology to discover, design and predict nanoscale morphologies within the field of complex soft matter that cannot be generated yet by other technology. We would like to mention that the arrangements of helical columns obtained by SOM are more complex than the bundles of helical proteins widely available in biology and known as coiled-coil proteins [7,8,125–127] or those obtained synthetically by more complex synthetic methodologies [128–133]. SOM provides a potential new entry to complex dynamic functional systems and materials [134–136]. Finally, the first application of SOM [137] provides the only methodology available today that can discriminate between the conical and crown conformers of self-assembling dendrimers during the self-organization of their spherical assemblies in a cubic lattice.

Author contributions

Virgil Percec: Conceptualization, Writing - Original Draft, Writing - Review & Editing, Supervision, Project administration, Funding acquisition. **Ning Huang**: Formal analysis, Investigation, Visualization. **Qi Xiao**: Formal analysis, Investigation, Resources, Visualization. **Benjamin E. Partridge**: Formal analysis, Investigation, Visualization. **Dipankar Sahoo**: Formal analysis, Investigation. **Mohammad R. Imam**: Resources. **Mihai Peterca**: Formal analysis, Investigation. **Robert Graf**: Formal analysis, Investigation. **Hans-Wolfgang Spiess**: Formal analysis, Investigation. **Xiangbing Zeng**:

Formal analysis, Visualization. **Goran Ungar**: Formal analysis, Investigation.

Declaration of Competing Interest

The authors declare that they have no known competing financial interests or personal relationships that could have appeared to influence the work reported in this paper.

Acknowledgment

Financial support by the National Science Foundation (DMR-1807127, DMR-1720530, and DMR- 2104554), the Humboldt Foundation, and the P. Roy Vagelos Chair at Penn (all to V.P.) is gratefully acknowledged. B.E.P. thanks the Howard Hughes Medical Institute for an International Student Research Fellowship. The authors thank Professor P. A. Heiney (University of Pennsylvania) for discussions of the XRD analysis. The authors acknowledge use of the Dual Source and Environmental X-ray Scattering (DEXS) facility operated by the Laboratory for Research on the Structure of Matter at the University of Pennsylvania (NSF MRSEC 1720530). The DEXS equipment purchase was made possible by an NSF MRI grant (1725969), an ARO DURIP grant (W911NF-17-1-0282), and the University of Pennsylvania. NMR Instrumentation (NEO400) was supported by the NSF Major Research Instrumentation Program (NSF CHE-1827457) and Vagelos Institute for Energy Science and Technology.

Supplementary materials

Supplementary material associated with this article can be found, in the online version, at doi:10.1016/j.giant.2021.100084.

References

[1] J.M. Lehn, Toward self-organization and complex matter, Science 295 (2002) 2400–2403, doi:10.1126/science.1071063.

[2] J.M. Lehn, Supramolecular chemistry: where from? where to? Chem. Soc. Rev. 46 (2017) 2378–2379, doi:10.1039/C7CS00115K.

[3] J.M. Lehn, Beyond chemical synthesis: self-organization, Isr. J. Chem. 58 (2018) 136–141, doi:10.1002/ijch.201800010.

[4] B.M. Rosen, C.J. Wilson, D.A. Wilson, M. Peterca, M.R. Imam, V. Percec, Dendron-mediated self-assembly, disassembly, and self-organization of complex systems, Chem. Rev. 109 (2009) 6275–6540, doi:10.1021/cr900157q.

[5] H.J. Sun, S. Zhang, V. Percec, From structure to function *via* complex supramolecular dendrimer systems, Chem. Soc. Rev. 44 (2015) 3900–3923, doi:10.1039/C4CS00249K.

[6] V. Percec, Merging macromolecular and supramolecular chemistry into bioinspired synthesis of complex systems, Isr. J. Chem. 60 (2020) 48–66, doi:10.1002/ijch.202000004.

[7] V. Percec, Q. Xiao, Helical self-organizations and emerging functions in architectures, biological and synthetic macromolecules, Bull. Chem. Soc. Jpn. 94 (2021) 900–928, doi:10.1246/bcsj.20210015.

[8] V. Percec, Q. Xiao, Helical chirality of supramolecular columns and spheres self-organizes complex liquid crystals, crystals, and quasicrystals, Isr. J. Chem. (2021) Published Online, doi:10.1002/ijch.202100057.

[9] V. Percec, From synthetic macromolecules to biological-like complex systems, in: V. Percec (Ed.), Hierarchical Macromolecular Structures: 60 Years After the Staudinger Nobel Prize I, 261, Springer International Publishing Ag, Cham, 2013, pp. 173–197. Advances in Polymer Science.

[10] B.M. Rosen, C. Roche, V. Percec, Self-assembly of dendritic dipeptides as a model of chiral selection in primitive biological systems, Top. Curr. Chem. 333 (2013) 213–253, doi:10.1007/128_2012_398.

[11] J. van der Gucht, Grand challenges in soft matter physics, Front. Phys. 6 (2018) 6–8, doi:10.3389/fphy.2018.00087.

[12] W. Jiang, Z. Qu, P. Kumar, D. Vecchio, Y. Wang, Y. Ma, J.H. Bahng, K. Bernardino, W.R. Gomes, F.M. Colombari, A. Lozada-Blanco, M. Veksler, E. Marino, A. Simon, C.B. Murray, S.Ricardo Muniz, A.F. De Moura, N.A. Kotov, Emergence of complexity in hierarchically organized chiral particles, Science 7949 (2020) 642–684, doi:10.1126/science.aaz7949.

[13] A. Lendlein, R. Langer, Biodegradable, elastic shape-memory polymers for potential biomedical applications, Science 296 (2002) 1673–1676, doi:10.1126/science.1066102.

[14] A. Lendlein, M. Balk, N.A. Tarazona, O.E.C. Gould, Bioperspectives for shape-memory polymers as shape programmable, active materials, Biomacromolecules 20 (2019) 3627–3640, doi:10.1021/acs.biomac.9b01074.

[15] T. Xie, Tunable polymer multi-shape memory effect, Nature 464 (2010) 267–270, doi:10.1038/nature08863.

[16] J.M. McCracken, B.R. Donovan, T.J. White, Materials as machines, Adv. Mater. 32 (2020) 1906564, doi:10.1002/adma.201906564.

[17] F. Serra, M. Buscaglia, T. Bellini, The emergence of memory in liquid crystals, Mater. Today 14 (2011) 488–494, doi:10.1016/S1369-7021(11)70213-9.

[18] Y. Furusho, T. Kimura, Y. Mizuno, T. Aida, Chirality-memory molecule: a D_2-symmetric fully substituted porphyrin as a conceptually new chirality sensor, J. Am. Chem. Soc. 119 (1997) 5267–5268, doi:10.1021/ja970431q.

[19] E. Yashima, K. Maeda, Y. Okamoto, Memory of macromolecular helicity assisted by interaction with achiral small molecules, Nature 399 (1999) 449–451, doi:10.1038/20900.

[20] F. Helmich, C.C. Lee, A.P.H.J. Schenning, E.W. Meijer, Chiral memory *via* chiral amplification and selective depolymerization of porphyrin aggregates, J. Am. Chem. Soc. 132 (2010) 16753–16755, doi:10.1021/ja1077602.

[21] T. Yuan, Z. Sun, A.U. Mu, M. Zeng, A.J. Kalin, Z. Cheng, M.A. Olson, L. Fang, Assembly and chiral memory effects of dynamic macroscopic supramolecular helices, Chem. Eur. J. 24 (2018) 16553–16557, doi:10.1002/chem.201803005.

[22] M. Peterca, M.R. Imam, S.D. Hudson, B.E. Partridge, D. Sahoo, P.A. Heiney, M.L. Klein, V. Percec, Complex arrangement of orthogonal nanoscale columns via a supramolecular orientational memory effect, ACS Nano 10 (2016) 10480–10488, doi:10.1021/acsnano.6b06419.

[23] D. Sahoo, M. Peterca, E. Aqad, B.E. Partridge, P.A. Heiney, R. Graf, H.W. Spiess, X. Zeng, V. Percec, Tetrahedral arrangements of perylene bisimide columns via supramolecular orientational memory, ACS Nano 11 (2017) 983–991, doi:10.1021/acsnano.6b07599.

[24] D. Sahoo, M. Peterca, E. Aqad, B.E. Partridge, M.L. Klein, V. Percec, Losing supramolecular orientational memory via self-organization of a misfolded secondary structure, Polym. Chem. 9 (2018) 2370–2381, doi:10.1039/C8PY00187A.

[25] N. Huang, M.R. Imam, M.J. Sienkowska, M. Peterca, M.N. Holerca, D.A. Wilson, B.M. Rosen, B.E. Partridge, Q. Xiao, V. Percec, Supramolecular spheres assembled from covalent and supramolecular dendritic crowns dictate the supramolecular orientational memory effect mediated by Frank-Kasper phases, Giant 1 (2020) 100001, doi:10.1016/j.giant.2020.100001.

[26] N. Huang, Q. Xiao, M. Peterca, X. Zeng, V. Percec, Self-Organisation of rhombitruncated cuboctahedral hexagonal columns from an amphiphilic Janus dendrimer, Mol. Phys. (2021) e1902586, doi:10.1080/00268976.2021.1902586.

[27] V.S.K. Balagurusamy, G. Ungar, V. Percec, G. Johansson, Rational design of the first spherical supramolecular dendrimers self-organized in a novel thermotropic cubic liquid-crystalline phase and the determination of their shape by X-ray analysis, J. Am. Chem. Soc. 119 (1997) 1539–1555, doi:10.1021/ja963295i.

[28] S.D. Hudson, H.T. Jung, V. Percec, W.D. Cho, G. Johansson, G. Ungar, V.S.K. Balagurusamy, Direct visualization of individual cylindrical and spherical supramolecular dendrimers, Science 278 (1997) 449–452, doi:10.1126/science.278.5337.449.

[29] V. Percec, C.H. Ahn, B. Barboiu, Self-encapsulation, acceleration and control in the radical polymerization of monodendritic monomers via self-assembly, J. Am. Chem. Soc. 119 (1997) 12978–12979, doi:10.1021/ja9727878.

[30] V. Percec, C.H. Ahn, G. Ungar, D.J.P. Yeardley, M. Möller, S.S. Sheiko, Controlling polymer shape through the self-assembly of dendritic side-groups, Nature 391 (1998) 161–164, doi:10.1038/34384.

[31] V. Percec, W.D. Cho, M. Möller, S.A. Prokhorova, G. Ungar, D.J.P. Yeardley, Design and structural analysis of the first spherical monodendron self-organizable in a cubic lattice, J. Am. Chem. Soc. 122 (2000) 4249–4250, doi:10.1021/ja9943400.

[32] D.R. Dukeson, G. Ungar, V.S.K. Balagurusamy, V. Percec, G.A. Johansson, M. Glodde, Application of isomorphous replacement in the structure determination of a cubic liquid crystal phase and location of counterions, J. Am. Chem. Soc. 125 (2003) 15974–15980, doi:10.1021/ja037380j.

[33] V. Percec, W.D. Cho, P.E. Mosier, G. Ungar, D.J.P. Yeardley, Structural analysis of cylindrical and spherical supramolecular dendrimers quantifies the concept of monodendron shape control by generation number, J. Am. Chem. Soc. 120 (1998) 11061–11070, doi:10.1021/ja9819007.

[34] V. Percec, C.H. Ahn, W.D. Cho, A.M. Jamieson, J. Kim, T. Leman, M. Schmidt, M. Gerle, M. Möller, S.A. Prokhorova, S.S. Sheiko, S.Z.D. Cheng, A. Zhang, G. Ungar, D.J.P. Yeardley, Visualizable cylindrical macromolecules with controlled stiffness from backbones containing libraries of self-assembling dendritic side groups, J. Am. Chem. Soc. 120 (1998) 8619–8631, doi:10.1021/ja981211v.

Full-length article

[35] G. Ungar, V. Percec, M.N. Holerca, G. Johansson, J.A. Heck, Heat-shrinking spherical and columnar supramolecular dendrimers: their interconversion and dependence of their shape on molecular taper angle, Chem. Eur. J. 6 (2000) 1258–1266 10.1002/(SICI)1521-3765(20000403)6:7<1258::AID-CHEM1258>3.0.CO;2-O.

[36] V. Percec, W.D. Cho, G. Ungar, D.J.P. Yeardley, From molecular flat tapers, discs, and cones to supramolecular cylinders and spheres using Fréchet-type monodendrons modified on their leriphery, Angew. Chem. Int. Ed. 39 (2000) 1597–1602 10.1002/(SICI)1521-3773(20000502)39:9<1597::AID-ANIE1597>3.0.CO;2-I.

[37] V. Percec, W.D. Cho, G. Ungar, Increasing the diameter of cylindrical and spherical supramolecular dendrimers by decreasing the solid angle of their monodendrons *via* periphery functionalization, J. Am. Chem. Soc. 122 (2000) 10273–10281, doi:10.1021/ja0024643.

[38] V. Percec, W.D. Cho, G. Ungar, D.J.P. Yeardley, Synthesis and structural analysis of two constitutional isomeric libraries of AB_2-based monodendrons and supramolecular dendrimers, J. Am. Chem. Soc. 123 (2001) 1302–1315, doi:10.1021/ja0037771.

[39] V. Percec, M.N. Holerca, S. Uchida, W.D. Cho, G. Ungar, Y. Lee, D.J.P. Yeardley, Exploring and expanding the three-dimensional structural diversity of supramolecular dendrimers with the aid of libraries of alkali metals of their AB_3 minidendritic carboxylates, Chem. Eur. J. 8 (2002) 1106–1117 10.1002/1521-3765(20020301)8:5<1106::AID-CHEM1106>3.0.CO;2-G.

[40] V. Percec, W.D. Cho, G. Ungar, D.J.P. Yeardley, Synthesis and NaOTf mediated self-assembly of monodendritic crown ethers, Chem. Eur. J. 8 (2002) 2011–2025 10.1002/1521-3765(20020503)8:9<2011::AID-CHEM2011>3.0.CO;2-3.

[41] V. Percec, M.N. Holerca, S. Uchida, D.J.P. Yeardley, G. Ungar, Poly(oxazoline)s with tapered minidendritic side groups as models for the design of synthetic macromolecules with tertiary structure. A demonstration of the limitations of living polymerization in the design of 3-D structures based on single polymer chains, Biomacromolecules 2 (2001) 729–740, doi:10.1021/bm015559l.

[42] A. Rapp, I. Schnell, D. Sebastiani, S.P. Brown, V. Percec, H.W. Spiess, Supramolecular assembly of dendritic polymers elucidated by ^{1}H and ^{13}C solid-state MAS NMR spectroscopy, J. Am. Chem. Soc. 125 (2003) 13284–13297, doi:10.1021/ja035127d.

[43] D.J.P. Yeardley, G. Ungar, V. Percec, M.N. Holerca, G. Johansson, Spherical supramolecular minidendrimers self-organized in an "inverse micellar"-like thermotropic body-centered cubic liquid crystalline hase, J. Am. Chem. Soc. 122 (2000) 1684–1689, doi:10.1021/ja993915q.

[44] H. Duan, S.D. Hudson, G. Ungar, M.N. Holerca, V. Percec, Definitive support by transmission electron microscopy, electron diffraction, and electron density maps for the formation of a BCC lattice from poly[N-[3,4,5-tris(n-dodecan-1-yloxy)benzoyl]ethyleneimine], Chem. Eur. J. 7 (2001) 4134–4141 10.1002/1521-3765(20011001)7:19<4134::aid-chem4134>3.0.co;2-w.

[45] F.C. Frank, J.S. Kasper, Complex alloy structures regarded as sphere packings. I. Definitions and basic principles, Acta Cryst. 11 (1958) 184–190, doi:10.1107/S0365110X58000487.

[46] F.C. Frank, J.S. Kasper, Complex alloy structures regarded as sphere packings. II. Analysis and classification of representative structures, Acta Cryst. 12 (1959) 483–499, doi:10.1107/S0365110X59001499.

[47] G. Ungar, Y. Liu, X. Zeng, V. Percec, W.D. Cho, Giant supramolecular liquid crystal lattice, Science 299 (2003) 1208–1211, doi:10.1126/science.1078849.

[48] X. Zeng, G. Ungar, Y. Liu, V. Percec, A.E. Dulcey, J.K. Hobbs, Supramolecular dendritic liquid quasicrystals, Nature 428 (2004) 157–160, doi:10.1038/nature02368.

[49] G. Ungar, V. Percec, X. Zeng, P. Leowanawat, Liquid quasicrystals, Isr. J. Chem. 51 (2011) 1206–1215, doi:10.1002/ijch.201100151.

[50] T. Dotera, Quasicrystals in soft matter, Isr. J. Chem. 51 (2011) 1197–1205, doi:10.1002/ijch.201100146.

[51] V. Percec, M.R. Imam, M. Peterca, W.D. Cho, P.A. Heiney, Self-assembling dendronized dendrimers, Isr. J. Chem. 49 (2009) 55–70, doi:10.1560/IJC.49.1.55.

[52] M. Peterca, M.R. Imam, P. Leowanawat, B.M. Rosen, D.A. Wilson, C.J. Wilson, X. Zeng, G. Ungar, P.A. Heiney, V. Percec, Self-assembly of hybrid dendrons into doubly segregated supramolecular polyhedral columns and vesicles, J. Am. Chem. Soc. 132 (2010) 11288–11305, doi:10.1021/ja104432d.

[53] B.M. Rosen, D.A. Wilson, C.J. Wilson, M. Peterca, B.C. Won, C. Huang, L.R. Lipski, X. Zeng, G. Ungar, P.A. Heiney, V. Percec, Predicting the structure of supramolecular dendrimers via the analysis of libraries of AB_3 and constitutional isomeric AB_2 biphenylpropyl ether self-assembling dendrons, J. Am. Chem. Soc. 131 (2009) 17500–17521, doi:10.1021/ja907882n.

[54] D.A. Wilson, K.A. Andreopoulou, M. Peterca, P. Leowanawat, D. Sahoo, B.E. Partridge, Q. Xiao, N. Huang, P.A. Heiney, V. Percec, Supramolecular spheres self-assembled from conical dendrons are chiral, J. Am. Chem. Soc. 141 (2019) 6162–6166, doi:10.1021/jacs.9b02206.

[55] V. Percec, M.R. Imam, M. Peterca, D.A. Wilson, R. Graf, H.W. Spiess, V.S.K. Balagurusamy, P.A. Heiney, Self-assembly of dendronized triphenylenes into helical pyramidal columns and chiral spheres, J. Am. Chem. Soc. 131 (2009) 7662–7677, doi:10.1021/ja8094944.

[56] V. Percec, M.R. Imam, M. Peterca, D.A. Wilson, P.A. Heiney, Self-assembly of dendritic crowns into chiral supramolecular spheres, J. Am. Chem. Soc 131 (2009) 1294–1304, doi:10.1021/ja8087778.

[57] B.M. Rosen, M. Peterca, C. Huang, X. Zeng, G. Ungar, V. Percec, Deconstruction as a strategy for the design of libraries of self-assembling dendrons, Angew. Chem. Int. Ed. 49 (2010) 7002–7005, doi:10.1002/anie.201002514.

[58] D. Sahoo, M. Peterca, E. Aqad, B.E. Partridge, P.A. Heiney, R. Graf, H.W. Spiess, X. Zeng, V. Percec, Hierarchical self-organization of perylene bisimides into supramolecular spheres and periodic arrays thereof, J. Am. Chem. Soc. 138 (2016) 14798–14807, doi:10.1021/jacs.6b09986.

[59] D. Sahoo, M.R. Imam, M. Peterca, B.E. Partridge, D.A. Wilson, X. Zeng, G. Ungar, P.A. Heiney, V. Percec, Hierarchical self-organization of chiral columns from chiral supramolecular spheres, J. Am. Chem. Soc. 140 (2018) 13478–13487, doi:10.1021/jacs.8b09174.

[60] M. Peterca, V. Percec, M.R. Imam, P. Leowanawat, K. Morimitsu, P.A. Heiney, Molecular structure of helical supramolecular dendrimers, J. Am. Chem. Soc. 130 (2008) 14840–14852, doi:10.1021/ja806524m.

[61] G. Ungar, X. Zeng, Frank Kasper, quasicrystalline and related phases in liquid crystals, Soft Matter 1 (2005) 95–106, doi:10.1039/B502443A.

[62] V. Percec, M. Peterca, M.J. Sienkowska, M.A. Ilies, E. Aqad, J. Smidrkal, P.A. Heiney, Synthesis and retrostructural analysis of libraries of AB_3 and constitutional isomeric AB_2 phenylpropyl ether-based supramolecular dendrimers, J. Am. Chem. Soc. 128 (2006) 3324–3334, doi:10.1021/ja060062a.

[63] V. Percec, C.M. Mitchell, W.D. Cho, S. Uchida, M. Glodde, G. Ungar, X. Zeng, Y. Liu, V.S.K. Balagurusamy, P.A. Heiney, Designing libraries of first generation AB_3 and AB_2 self-assembling dendrons *via* the primary structure generated from combinations of $(AB)_y{-}AB_3$ and $(AB)_y{-}AB_2$ building blocks, J. Am. Chem. Soc. 126 (2004) 6078–6094, doi:10.1021/ja049846j.

[64] V. Percec, M.N. Holerca, S. Nummelin, J.J. Morrison, M. Glodde, J. Smidrkal, M. Peterca, B.M. Rosen, S. Uchida, V.S.K. Balagurusamy, M.J. Sienkowska, P.A. Heiney, Exploring and expanding the structural diversity of self-assembling dendrons through combinations of AB, constitutional isomeric AB_2, and AB_3 biphenyl-4-methyl ether building blocks, Chem. Eur. J. 12 (2006) 6216–6241, doi:10.1002/chem.200600178.

[65] V. Percec, B.C. Won, M. Peterca, P.A. Heiney, Expanding the structural diversity of self-assembling dendrons and supramolecular dendrimers via complex building blocks, J. Am. Chem. Soc. 129 (2007) 11265–11278, doi:10.1021/ja073714j.

[66] V. Percec, J.G. Rudick, M. Peterca, M.E. Yurchenko, J. Smidrkal, P.A. Heiney, Supramolecular structural diversity among first-generation hybrid dendrimers and twin dendrons, Chem. Eur. J. 14 (2008) 3355–3362, doi:10.1002/chem.200701658.

[67] V. Percec, M. Peterca, Y. Tsuda, B.M. Rosen, S. Uchida, M.R. Imam, G. Ungar, P.A. Heiney, Elucidating the structure of the Pm3n cubic phase of supramolecular dendrimers through the modification of their aliphatic to aromatic volume ratio, Chem. Eur. J. 15 (2009) 8994–9004, doi:10.1002/chem.200901324.

[68] V. Percec, M. Peterca, A.E. Dulcey, M.R. Imam, S.D. Hudson, S. Nummelin, P. Adelman, P.A. Heiney, Hollow spherical supramolecular dendrimers, J. Am. Chem. Soc. 130 (2008) 13079–13094, doi:10.1021/ja8034703.

[69] M.R. Imam, M. Peterca, U. Edlund, V.S.K. Balagurusamy, V. Percec, Dendronized supramolecular polymers self-assembled from dendritic ionic liquids, J. Polym. Sci. Part A Polym. Chem. 47 (2009) 4165–4193, doi:10.1002/pola.23523.

[70] V. Percec, C. Grigoras, H.J. Kim, Toward self-assembling dendritic macromolecules from conventional monomers by a combination of living radical polymerization and irreversible terminator multifunctional initiator, J. Polym. Sci. Part A Polym. Chem. 42 (2004) 505–513, doi:10.1002/pola.11014.

[71] M.N. Holerca, D. Sahoo, M. Peterca, B.E. Partridge, P.A. Heiney, V. Percec, A tetragonal phase self-organized from unimolecular spheres assembled from a substituted poly(2-oxazoline), Macromolecules 50 (2017) 375–385, doi:10.1021/acs.macromol.6b02298.

[72] M.N. Holerca, D. Sahoo, B.E. Partridge, M. Peterca, X. Zeng, G. Ungar, V. Percec, Dendronized poly(2-oxazoline) displays within only five monomer repeat units liquid quasicrystal, A15 and σ Frank–Kasper phases, J. Am. Chem. Soc. 140 (2018) 16941–16947, doi:10.1021/jacs.8b11103.

[73] M.N. Holerca, M. Peterca, B.E. Partridge, Q. Xiao, G. Lligadas, M.J. Monteiro, V. Percec, Monodisperse macromolecules by self-interrupted living polymerization, J. Am. Chem. Soc. 142 (2020) 15265–15270, doi:10.1021/jacs.0c07912.

[74] V. Percec, A.E. Dulcey, V.S.K. Balagurusamy, Y. Miura, J. Smidrkal, M. Peterca, S. Nummelin, U. Edlund, S.D. Hudson, P.A. Heiney, H. Duan, S.N. Magonov, S.A. Vinogradov, Self-assembly of amphiphilic dendritic dipeptides into helical pores, Nature 430 (2004) 764–768, doi:10.1038/nature02770.

[75] V. Percec, A.E. Dulcey, M. Peterca, M. Ilies, S. Nummelin, M.J. Sienkowska, P.A. Heiney, Principles of self-assembly of helical pores from dendritic dipeptides, Proc. Natl. Acad. Sci. U.S.A. 103 (2006) 2518–2523, doi:10.1073/pnas.0509676103.

[76] V. Percec, J. Smidrkal, M. Peterca, C.M. Mitchell, S. Nummelin, A.E. Dulcey, M.J. Sienkowska, P.A. Heiney, Self-assembly of hybrid dendrons with complex primary structure into functional helical pores, Chem. A Eur. J. 13 (2007) 3989–4007, doi:10.1002/chem.200601582.

[77] M.S. Kaucher, M. Peterca, A.E. Dulcey, A.J. Kim, S.A. Vinogradov, D.A. Hammer, P.A. Heiney, V. Percec, Selective transport of water mediated by porous dendritic dipeptides, J. Am. Chem. Soc. 129 (2007) 11698–11699, doi:10.1021/ja076066c.

[78] V. Percec, A.E. Dulcey, M. Peterca, P. Adelman, R. Samant, V.S.K. Balagurusamy, P.A. Heiney, Helical pores self-assembled from homochiral dendritic dipeptides based on l-Tyr and nonpolar alpha-amino acids, J. Am. Chem. Soc. 129 (2007) 5992–6002, doi:10.1021/ja071088k.

[79] C. Roche, H.J. Sun, P. Leowanawat, F. Araoka, B.E. Partridge, M. Peterca, D.A. Wilson, M.E. Prendergast, P.A. Heiney, R. Graf, H.W. Spiess, X. Zeng, G. Ungar, V. Percec, A supramolecular helix that disregards chirality, Nat. Chem. 8 (2016) 80–89, doi:10.1038/nchem.2397.

[80] B.E. Partridge, L. Wang, D. Sahoo, J.T. Olsen, P. Leowanawat, C. Roche, H. Ferreira, K.J. Reilly, X. Zeng, G. Ungar, P.A. Heiney, R. Graf, H.W. Spiess, V. Percec, Sequence-defined dendrons dictate supramolecular cogwheel assembly of dendronized perylene bisimides, J. Am. Chem. Soc. 141 (2019) 15761–15766, doi:10.1021/jacs.9b08714.

[81] L. Wang, B.E. Partridge, N. Huang, J.T. Olsen, D. Sahoo, X. Zeng, G. Ungar, R. Graf, H.W. Spiess, V. Percec, Extraordinary acceleration of cogwheel helical self-organization of dendronized perylene bisimides by the dendron sequence encoding their tertiary structure, J. Am. Chem. Soc. 142 (2020) 9525–9536, doi:10.1021/jacs.0c03353.

[82] C. Roche, H.J. Sun, M.E. Prendergast, P. Leowanawat, B.E. Partridge, P.A. Heiney, F. Araoka, R. Graf, H.W. Spiess, X. Zeng, G. Ungar, V. Percec, Homochiral columns constructed by chiral self-sorting during supramolecular helical organization of hat-ahaped molecules, J. Am. Chem. Soc. 136 (2014) 7169–7185, doi:10.1021/ja5035107.

[83] Y.K. Kwon, S. Chvalun, A.I. Schneider, J. Blackwell, V. Percec, J.A. Heck, Supramolecular tubular structures of a polymethacrylate with tapered side groups in aligned hexagonal phases, Macromolecules 27 (1994) 6129–6132, doi:10.1021/ma00099a029.

[84] V. Percec, D. Schlueter, G. Ungar, S.Z.D. Cheng, A. Zhang, Hierarchical control of internal superstructure, diameter, and stability of supramolecular and macromolecular columns generated from tapered monodendritic building blocks, Macromolecules 31 (1998) 1745–1762, doi:10.1021/ma971459p.

[85] V. Percec, P. Leowanawat, Why are biological systems homochiral? Isr. J. Chem. 51 (2011) 1107–1117, doi:10.1002/ijch.201100152.

[86] V. Percec, Guest editorial: origin, transfer, and amplification of chirality, Isr. J. Chem. 51 (2011) 989 989, doi:10.1002/ijch.201100103.

[87] Y. Li, S.T. Lin, W.A. Goddard, Efficiency of various lattices from hard ball to soft ball: theoretical study of thermodynamic properties of dendrimer liquid crystal from atomistic simulation, J. Am. Chem. Soc. 126 (2004) 1872–1885, doi:10.1021/ja038617e.

[88] P. Ziherl, R.D. Kamien, Maximizing entropy by minimizing area: Towards a new principle of self-organization, J. Phys. Chem. B 105 (2001) 10147–10158, doi:10.1021/jp010944q.

[89] C.R. Iacovella, A.S. Keys, S.C. Glotzer, Self-assembly of soft-matter quasicrystals and their approximants, Proc. Natl. Acad. Sci. U.S.A. 108 (2011) 20935–20940, doi:10.1073/pnas.1019763108.

[90] S. Lee, M.J. Bluemle, F.S. Bates, Discovery of a Frank-Kasper σ phase in sphere-forming block copolymer melts, Science 330 (2010) 349–353, doi:10.1126/science.1195552.

[91] S. Fischer, A. Exner, K. Zielske, J. Perlich, S. Deloudi, W. Steurer, P. Lindner, S. Förster, Colloidal quasicrystals with 12-fold and 18-fold diffraction symmetry, Proc. Natl. Acad. Sci. U. S. A. 108 (2011) 1810–1814, doi:10.1073/pnas.1008695108.

[92] J. Zhang, F.S. Bates, Dodecagonal quasicrystalline morphology in a poly(styrene-b-isoprene-b-styrene-b-ethylene oxide) tetrablock terpolymer, J. Am. Chem. Soc. 134 (2012) 7636–7639, doi:10.1021/ja301770v.

[93] T.M. Gillard, S. Lee, F.S. Bates, Dodecagonal quasicrystalline order in a diblock copolymer melt, Proc. Natl. Acad. Sci. U.S.A. 113 (2016) 5167–5172, doi:10.1073/pnas.1601692113.

[94] K. Kim, M.W. Schulze, A. Arora, R.M. Lewis, M.A. Hillmyer, K.D. Dorfman, F.S. Bates, Thermal processing of diblock copolymer melts mimics metallurgy, Science 356 (2017) 520–523, doi:10.1126/science.aam7212.

[95] Y. Sun, R. Tan, Z. Ma, Z. Gan, G. Li, D. Zhou, Y. Shao, W.B. Zhang, R. Zhang, X.H. Dong, Discrete block copolymers with diverse architectures: resolving complex spherical phases with one monomer resolution, ACS Cent. Sci. 6 (2020) 1386–1393, doi:10.1021/acscentsci.0c00798.

[96] M. Peterca, V. Percec, Recasting metal alloy phases with block copolymers, Science 330 (2010) 330–334, doi:10.1126/science.1196698.

[97] D.V. Perroni, M.K. Mahanthappa, Inverse *Pm*3*n*, cubic micellar lyotropic phases from zwitterionic triazolium gemini surfactants, Soft Matter 9 (2013) 7919–7922, doi:10.1039/C3SM51238J.

[98] S.A. Kim, K.J. Jeong, A. Yethiraj, M.K. Mahanthappa, Low-symmetry sphere packings of simple surfactant micelles induced by ionic sphericity, Proc. Natl. Acad. Sci. U.S.A. 114 (2017) 4072–4077, doi:10.1073/pnas.1701608114.

[99] C.M. Baez-Cotto, M.K. Mahanthappa, Micellar mimicry of intermetallic C14 and C15 laves phases by aqueous lyotropic self-assembly, ACS Nano 12 (2018) 3226–3234, doi:10.1021/acsnano.7b07475.

[100] A. Jayaraman, D.Y. Zhang, B.L. Dewing, M.K. Mahanthappa, Path-dependent preparation of complex micelle packings of a hydrated diblock oligomer, ACS Cent. Sci. 5 (2019) 619–628, doi:10.1021/acscentsci.8b00903.

[101] M. Huang, C.H. Hsu, J. Wang, S. Mei, X. Dong, Y. Li, M. Li, H. Liu, W. Zhang, T. Aida, W.B. Zhang, K. Yue, S.Z.D. Cheng, Selective assemblies of giant tetrahedra via precisely controlled positional interactions, Science 348 (2015) 424–428, doi:10.1126/science.aaa2421.

[102] K. Yue, M. Huang, R.L. Marson, J. He, J. Huang, Z. Zhou, J. Wang, C. Liu, X. Yan, K. Wu, Z. Guo, H. Liu, W. Zhang, P. Ni, C. Wesdemiotis, W.B. Zhang, S.C. Glotzer, S.Z.D. Cheng, Geometry induced sequence of nanoscale Frank–Kasper and quasicrystal mesophases in giant surfactants, Proc. Natl. Acad. Sci. U.S.A. 113 (2016) 14195–14200, doi:10.1073/pnas.1609422113.

[103] X. Feng, R. Zhang, Y. Li, Y. Hong, D. Guo, K. Lang, K.Y. Wu, M. Huang, J. Mao, C. Wesdemiotis, Y. Nishiyama, W. Zhang, W. Zhang, T. Miyoshi, T. Li, S.Z.D. Cheng, Hierarchical self-organization of AB_n dendron-like molecules into a supramolecular lattice sequence, ACS Cent. Sci. 3 (2017) 860–867, doi:10.1021/acscentsci.7b00188.

[104] X. Feng, R. Zhang, Y. Li, Y. Hong, D. Guo, K. Lang, K.Y. Wu, M. Huang, J. Mao, C. Wesdemiotis, Y. Nishiyama, W. Zhang, W. Zhang, T. Miyoshi, T. Li, S.Z.D. Cheng, Hierarchical self-organization of AB_n dendron-like molecules into a supramolecular lattice sequence, ACS Cent. Sci. 3 (2017) 860–867, doi:10.1021/acscentsci.7b00188.

[105] Z. Su, C.H. Hsu, Z. Gong, X. Feng, J. Huang, R. Zhang, Y. Wang, J. Mao, C. Wesdemiotis, T. Li, S. Seifert, W. Zhang, T. Aida, M. Huang, S.Z.D. Cheng, Identification of a Frank–Kasper Z phase from shape amphiphile self-assembly, Nat. Chem. 11 (2019) 899–905, doi:10.1038/s41557-019-0330-x.

[106] Y. Liu, T. Liu, X. Yan, Q.Y. Guo, J. Wang, R. Zhang, S. Zhang, Z. Su, J. Huang, G.X. Liu, W. Zhang, W. Zhang, T. Aida, K. Yue, M. Huang, S.Z.D. Cheng, Mesoatom alloys *via* self-sorting approach of giant molecules blends, Giant 4 (2020) 100031, doi:10.1016/j.giant.2020.100031.

[107] P. Mariani, V. Luzzati, H. Delacroix, Cubic phases of lipid-containing systems: structure analysis and biological implications, J. Mol. Biol. 204 (1988) 165–189, doi:10.1016/0022-2836(88)90607-9.

[108] R. Vargas, P. Mariani, A. Gulik, V. Luzzati, Cubic phases of lipid-containing systems: the structure of phase Q223 (space group Pm3n). An X-ray scattering study, J. Mol. Biol. 225 (1992) 137–145, doi:10.1016/0022-2836(92)91031-j.

[109] J. Charvolin, J.F. Sadoc, Periodic systems of frustrated fluid films and « micellar » cubic structures in liquid crystals, J. Phys. Fr. 49 (1988) 521–526, doi:10.1051/jphys:01988004903052100.

[110] L. Paccamiccio, M. Pisani, F. Spinozzi, C. Ferrero, S. Finet, P. Mariani, Pressure effects on lipidic direct phases: the dodecyl trimethyl ammonium chloride−water system, J. Phys. Chem. B 110 (2006) 12410–12418, doi:10.1021/jp054467d.

[111] M. Bastos, T. Silva, V. Teixeira, K. Nazmi, J.G.M. Bolscher, S.S. Funari, D. Uhríková, Lactoferrin-derived antimicrobial peptide induces a micellar cubic phase in a model membrane system, Biophys. J. 101 (2011) L20–L22, doi:10.1016/j.bpj.2011.06.038.

[112] T. Silva, R. Adão, K. Nazmi, J.G.M. Bolscher, S.S. Funari, D. Uhríková, M. Bastos, Structural diversity and mode of action on lipid membranes of three lactoferrin candidacidal peptides, Biochim. Biophys. Acta. Biomembr. 1828 (2013) 1329–1339, doi:10.1016/j.bbamem.2013.01.022.

[113] H. Delacroix, T. Gulik-Krzywicki, P. Mariani, V. Luzzati, Freeze-fracture electron microscope study of lipid systems: the cubic phase of space group Pm3n, J. Mol. Biol. 229 (1993) 526–539, doi:10.1006/jmbi.1993.1052.

[114] G.C. Shearman, A.I.I. Tyler, N.J. Brooks, R.H. Templer, O. Ces, R.V. Law, J.M. Seddon, Ordered micellar and inverse micellar lyotropic phases, Liq. Cryst. 37 (2010) 679–694, doi:10.1080/02678292.2010.484917.

[115] D.V. Talapin, E.V. Shevchenko, M.I. Bodnarchuk, X. Ye, J. Chen, C.B. Murray, Quasicrystalline order in self-assembled binary nanoparticle superlattices, Nature 461 (2009) 964–967, doi:10.1038/nature08439.

[116] X. Ye, J. Chen, M.Eric Irrgang, M. Engel, A. Dong, S.C. Glotzer, C.B. Murray, Quasicrystalline nanocrystal superlattice with partial matching rules, Nat. Mater. 16 (2016) 214–219, doi:10.1038/nmat4759.

[117] M. Girard, S. Wang, J.S. Du, A. Das, Z. Huang, V.P. Dravid, B. Lee, C.A. Mirkin, M.O. de la Cruz, Particle analogs of electrons in colloidal crystals, Science 364 (2019) 1174–1178, doi:10.1126/science.aaw8237.

[118] K.K. Lachmayr, C.M. Wentz, L.R. Sita, An exceptionally stable and scalable sugar–polyolefin Frank–Kasper A15 phase, Angew. Chem. Int. Ed. 59 (2020) 1521–1526, doi:10.1002/anie.201912648.

[119] K.K. Lachmayr, L.R. Sita, Small-molecule modulation of soft-matter Frank-Kasper phases: a method for adding function to form, Angew. Chem. Int. Ed. 59 (2020) 3563–3567, doi:10.1002/anie.201915416.

[120] A.P. Hynninen, J.H.J. Thijssen, E.C.M. Vermolen, M. Dijkstra, A. van Blaaderen, Self-assembly route for photonic crystals with a bandgap in the visible region, Nat. Mater. 6 (2007) 202–205, doi:10.1038/nmat1841.

[121] É. Ducrot, M. He, G.R. Yi, D.J. Pine, Colloidal alloys with preassembled clusters and spheres, Nat. Mater. 16 (2017) 652–657, doi:10.1038/nmat4869.

[122] Y. Wang, I.C. Jenkins, J.T. McGinley, T. Sinno, J.C. Crocker, Colloidal crystals with diamond symmetry at optical lengthscales, Nat. Commun. 8 (2017) 14173, doi:10.1038/ncomms14173.

[123] N. Zhang, S.R. Samanta, B.M. Rosen, V. Percec, Single electron transfer in radical ion and radical-mediated organic, materials and polymer synthesis, Chem. Rev. 114 (2014) 5848–5958, doi:10.1021/cr400689s.

[124] P.A. Heiney, Datasqueeze: a software tool for powder and small-angle X-ray diffraction analysis, Comm. Powder Diffr. Newslett. 32 (2005) 9–11.

[125] L. Pauling, L R.B. Corey, Compound helical configurations of polypeptide chains: structure of proteins of the α-keratin type, Nature 171 (1953) 59–61, doi:10.1038/171059a0.

[126] F.H.C. Crick, The packing of α-helices: simple coiled-coils, Acta. Cryst. 6 (1953) 689–697, doi:10.1107/S0365110X53001964.

[127] E. Moutevelis, D.N.A. Woolfson, Periodic table of coiled-coil protein structures, J. Mol. Biol. 385 (2009) 726–732, doi:10.1016/j.jmb.2008.11.028.

[128] V. Percec, C.H. Ahn, T.K. Bera, G. Ungar, D.J.P. Yeardley, Coassembly of a hexagonal columnar liquid crystalline superlattice from polymer(s) coated with a three-cylindrical bundle supramolecular dendrimer, Chem. Eur. J. 5 (1999) 1070–1083, doi:10.1002/(SICI)1521-3765(19990301)5:3-1070::AID-CHEM1070-3.0.CO;2-9.

[129] V. Percec, T.K. Bera, M. Glodde, Q. Fu, V.S.K. Balagurusamy, P.A. Heiney, Hierarchical self-assembly, coassembly, and self-organization of novel liquid crystalline lattices and superlattices from a twin-tapered dendritic benzamide and its four-cylinder-bundle supramolecular polymer, Chem. Eur. J. 9 (2003) 921–935, doi:10.1002/chem.200390114.

[130] V. Percec, M.R. Imam, M. Peterca, P. Leowanawat, Self-organizable vesicular columns assembled from polymers dendronized with semifluorinated Janus dendrimers act as reverse thermal actuators, J. Am. Chem. Soc. 134 (2012) 4408–4420, doi:10.1021/ja2118267.

[131] J.E. Marine, Song S, X. Liang, M.D. Watson, J.G. Rudick, Bundle-forming α-helical peptide–dendron hybrid, Chem. Commun. 51 (2015) 14314–14317, doi:10.1039/C5CC05468K.

[132] J.E. Marine, S. Song, X. Liang, J.G. Rudick, Synthesis and self-assembly of bundle-forming α-helical eptide–dendron hybrids, Biomacromolecules 17 (2016) 336–344, doi:10.1021/acs.biomac.5b01452.

[133] D.A. Barkley, Y. Rokhlenko, J.E. Marine, R. David, D. Sahoo, M.D. Watson, T. Koga, C.O. Osuji, J.G. Rudick, Hexagonally ordered arrays of α-helical bundles formed from peptide-dendron hybrids, J. Am. Chem. Soc. 139 (2017) 15977–15983, doi:10.1021/jacs.7b09737.

[134] C. Roche, V. Percec, Complex adaptable systems based on self-assembling dendrimers and dendrons: toward dynamic materials, Isr. J. Chem. 53 (2013) 30–44, doi:10.1002/ijch.201200099.

[135] J.M. Lehn, From supramolecular chemistry towards conctitutional dynamic chemistry and adaptive chemistry, Chem. Soc. Rev. 36 (2007) 151–160, doi:10.1039/B616752G.

[136] M. Barboiu, J.M. Lehn, Dynamic chemical devices: modulation of contraction/extension molecular motion by coupled-ion binding/pH change-induced structural switching, Proc. Natl. Acad. Sci. U.S.A. 99 (2002) 5201–5206, doi:10.1073/pnas.082099199.

[137] V. Percec, S. Wang, N. Huang, B.E. Partridge, X. Wang, D. Sahoo, D.J. Hoffman, J. Malineni, M. Peterca, R.L. Jezorek, N. Zhang, H. Daud, P.D. Sung, E.R. McClure, S.L. Song, An accelerated modular-orthogonal Ni-catalyzed methodology to symmetric and nonsymmetric constitutional isomeric AB_2 to AB_9 dendrons exhibiting unprecedented self-organizing principles, J. Am. Chem. Soc. 143 (2021) 17724–17743, doi:10.1021/jacs.1c08502.